

Supporting Information

Leveraging bile solubilization of poorly water-soluble drugs by rational polymer selection

Figures:	2
Tables:.....	4
S1 Methods	5
S2 ¹ H nuclear magnetic resonance (NMR) data interpretation.....	6
S3 Polymer characterization in TC/L in PBS and in PBS	11
S3.1 Particle size analysis in PBS by dynamic light scattering (DLS)	11
S3.2 ¹ H nuclear magnetic resonance (¹ H NMR) analysis of polymers	14
S3.2.1 Colesevelam in PBS.....	15
S3.2.2 Colesevelam in TC/L in PBS	16
S3.2.3 Eudragit E in PBS.....	17
S3.2.4 Eudragit E in TC/L in PBS	18
S3.2.5 Soluplus in PBS.....	19
S3.2.6 Soluplus in TC/L in PBS	20
S3.2.7 Kollidon VA 64 in PBS.....	21
S3.2.8 Kollidon VA 64 in TC/L in PBS	22
S3.2.9 HPMC-AS in PBS	23
S3.2.10 HPMC-AS in TC/L in PBS	24
S3.2.11 Complete ¹ H NMR spectra	25
S4 Polymer impact on free drug	26
S4.1 Perphenazine ¹ H nuclear magnetic resonance (¹ H NMR) analysis	26
S4.2 Imatinib ¹ H nuclear magnetic resonance (¹ H NMR) analysis	29
S4.3 Metoprolol ¹ H nuclear magnetic resonance (¹ H NMR) analysis.....	31
S5 Polymer impact on HDO diffusivity	32
S6 Excipient concentration under physiological conditions	33
S7 Flux evaluation.....	34
S7.1 Flux at different TC/L concentrations.....	34
S7.2 Flux at different drug starting concentrations	35
S7.3 Drug concentration over time	36
S7.4 Flux lag time	42
S7.4.1 Lag time Perphenazine	42
S7.4.2 Lag time Imatinib	44
S7.4.3 Lag time Metoprolol.....	46
S8 Imatinib flux reduction by polymer presence	46



Figures:

Figure S1: Flux assay as described in 2.2.3	5
Figure S2: HPLC calibration spectra for (A) Perphenazine, (B) Imatinib, and (C) Metoprolol. Signal area under the curve (AUC) increased linearly with concentration. Respective nominal drug concentrations are shown on the right side of each spectrum. λ represents wavelength of detector and t_{ret} retention time of respective drug peak.	5
Figure S3: ¹ H NMR signal assignment of taurocholate (TC) and lecithin (L) based on [1].	6
Figure S4: Complete ¹ H NMR spectra of Metoprolol, Imatinib, and Perphenazine with TC/L. Bottom shows TC/L reference spectrum.	6
Figure S5: Complete ¹ H NMR spectrum with signal assignment and respective molecular structure of Metoprolol in PBS. Standard 1D and 2D NMR techniques were applied for signal assignment.	7
Figure S6: Complete ¹ H NMR spectrum with signal assignment and respective molecular structure of Imatinib in PBS. Standard 1D and 2D NMR techniques were applied for signal assignment.	8
Figure S7: Complete ¹ H NMR spectrum with signal assignment and respective molecular structure of Perphenazine in PBS. Standard 1D and 2D NMR techniques were applied for signal assignment.	9
Figure S8: Interpretation of the NMR spectral patterns of the aryl-proton signals of drug molecules without polymer in PBS (A) and in TC/L in PBS (B) and with polymer in PBS (C) and in TC/L in PBS (D).	10
Figure S9: Mean hydrodynamic diameters of colloids in PBS (grey) and in TC/L in PBS (red) with (A) Colesevelam, (B) Eudragit E, (C) Soluplus, (D) Kollidon VA 64, and (E) HPMC-AS at different concentrations by DLS (mean \pm SD). At $\geq 0.5\%$ Colesevelam particles were detected (A grey). Turbidity was also observed for Eudragit E at 0.01, 0.5, and 1% (B, grey). At 0.05 and 0.1% Eudragit E formed colloids around 20 nm. Conversely, Eudragit E in TC/L in PBS formed colloids at $\geq 0.05\%$ (B, red). Soluplus formed 60-90 nm particles in PBS (C, grey). At $\geq 0.1\%$ Kollidon VA 64 particles around 40 nm were observed (D, grey). Hydrodynamic diameters of HPMC-AS ranged from 70 to 250 nm at 0.05 and 0.1% (E, grey). At $\geq 0.5\%$ particle size up to 500 nm were observed along with turbidity.	11
Figure S10: Chemical structures of used polymers.	14
Figure S11: ¹ H NMR spectra of Colesevelam at 0.01, 0.05, 0.1, 0.5, and 1% in PBS. No Colesevelam signals were detected.	15
Figure S12: ¹ H NMR spectra of Colesevelam at 0.01, 0.05, 0.1, 0.5, and 1% in TC/L in PBS indicated as (L) green lines and (TC) red lines. TC/L reference spectrum is shown (bottom). TC/L signal intensities decreased as a function of Colesevelam concentration. At $\geq 0.1\%$ signals sharpened (e.g. TC H25 and H26). At $\geq 0.5\%$ sharp TC signals with low intensity were found indicating precipitation of TC/L. Few TC remains in solution, but does not aggregate.	16
Figure S13: ¹ H NMR spectra of Eudragit E at 0.01, 0.05, 0.1, 0.5, and 1% in PBS. Sharp signals with low intensity were detected at 0.01%. At $\geq 0.05\%$, broad Eudragit E signals were observed. Some sharp signals shifted to lower ppm dependent on concentration (e.g. at 2.8 ppm).	17
Figure S14: ¹ H NMR spectra of Eudragit E at 0.01, 0.05, 0.1, 0.5, and 1% in TC/L in PBS indicated as (L) green lines and (TC) red lines. TC/L reference spectrum is shown (bottom). At 0.01% L signals disappeared, while TC signals sharpened. At $\geq 0.05\%$ L signals reappeared. At $\geq 0.1\%$ some TC/L signals shifted and at $\geq 0.5\%$ disappeared (e.g. TC H21, H19, and 18). Other signals did not disappear, but intensity decreased along with signal broadening (e.g. L H4, TC H26).	18
Figure S15: ¹ H NMR spectra of Soluplus at 0.01, 0.05, 0.1, 0.5 and 1% in PBS. Signal intensity increased as a function of concentration. Broad signals (e.g. at 1.3-2.6 ppm) and sharp signals (e.g. at 1.1 and 1.9 ppm) were detected in parallel.	19
Figure S16: ¹ H NMR spectra of Soluplus at 0.01, 0.05, 0.1, 0.5 and 1% in TC/L in PBS indicated as (L) green lines and (TC) red lines. TC/L reference spectrum is shown (bottom). At 1% some TC signals appeared very broad (e.g. TC H12, H7, H25, H3, H21, H19, and H18). Other signals were still observed (e.g. all L and TC H26).	20
Figure S17: ¹ H NMR spectra of Kollidon VA 64 at 0.01, 0.05, 0.1, 0.5 and 1% in PBS. Signal intensity increased as a function of concentration. Broad signals (e.g. at 1.6-2.5 ppm) were detected.	21

Figure S18: ¹ H NMR spectra of Kollidon VA 64 at 0.01, 0.05, 0.1, 0.5 and 1% in TC/L in PBS indicated as (L) green lines and (TC) red lines. TC/L reference spectrum is shown (bottom). TC/L signals did not change. Kollidon VA 64 signals increased as a function of concentration overlapping with TC/L signals.	22
Figure S19: ¹ H NMR spectra of HPMC-AS at 0.01, 0.05, 0.1, 0.5 and 1% in PBS. Signal intensity increased as a function of concentration. Broad signals (e.g. at 3.0-4.0 ppm) were detected along with sharp signals (e.g. at 1.9 and 2.4 ppm).	23
Figure S20: (A) ¹ H NMR spectra of HPMC-AS at 0.01, 0.05, 0.1, 0.5 and 1% in TC/L in PBS indicated as (L) green lines and (TC) red lines. TC/L reference spectrum is shown (bottom). (B) Overlay of 1% HPMC-AS with TC/L and TC/L reference spectrum (B). TC/L signals did not change. HPMC-AS signals increased as a function of concentration and overlapped TC/L signals.	24
Figure S21: ¹ H NMR spectra of 1% Colesevelam, Eudragit E, Soluplus, Kollidon VA 64, and HPMC-AS in TC/L in PBS.	25
Figure S22: Complete ¹ H NMR spectra of 1% Colesevelam, Eudragit E, Soluplus, Kollidon VA 64, and HPMC-AS in PBS.	26
Figure S23: Complete ¹ H NMR spectra of Colesevelam with Perphenazine in TC/L in PBS and in PBS.	26
Figure S24: Complete ¹ H NMR spectra of Eudragit E with Perphenazine in PBS in TC/L and in PBS.	27
Figure S25: Complete ¹ H NMR spectra of Soluplus with Perphenazine in PBS in TC/L and in PBS.	27
Figure S26: Complete ¹ H NMR spectra of Kollidon VA 64 with Perphenazine in PBS in TC/L and in PBS.	28
Figure S27: Complete ¹ H NMR spectra of HPMC-AS with Perphenazine in PBS in TC/L and in PBS.	28
Figure S28: Complete ¹ H NMR spectra of Colesevelam with Imatinib in PBS in TC/L and in PBS.	29
Figure S29: complete ¹ H NMR spectra of Eudragit E with Imatinib in PBS in TC/L and in PBS.	29
Figure S30: Complete ¹ H NMR spectra of Soluplus with Imatinib in PBS in TC/L and in PBS.	30
Figure S31: Complete ¹ H NMR spectra of Kollidon VA 64 with Imatinib in PBS in TC/L and in PBS.	30
Figure S32: Complete ¹ H NMR spectra of HPMC-AS with Imatinib in PBS in TC/L and in PBS.	31
Figure S33: Metoprolol ¹ H NMR aryl-proton spectra (A) in TC/L in PBS and with 1% respective polymer in TC/L in PBS (B-F). Metoprolol aryl-proton signals were not impacted by (B) Colesevelam, (C) Eudragit E, (E) Kollidon VA 64, and (F) HPMC-AS at 1% in TC/L in PBS. (D) Signal decreased in intensity and broadened by Soluplus.	31
Figure S34: Metoprolol ¹ H NMR aryl-proton spectra (A) in PBS and with 1% respective polymer in PBS (B-F). (B) Colesevelam, (C) Eudragit E, (D) Soluplus and (E) Kollidon VA 64 decreased signal intensity in PBS. (D) Soluplus broadened signals. (F) Signals were not impacted by 1% HPMC-AS in PBS.	32
Figure S35: DOSY analysis: (A) HDO (4.703 ppm) signal attenuation with increased gradient strength and (B) fitted curve of experimental intensity decay as a function of the gradient strength for Perphenazine in TC/L in PBS (without polymer).	33
Figure S36: Flux of (A) Perphenazine, (B) Imatinib, and (C) Metoprolol (each at 1000 μmol/l) in PBS (black), in TC/L in PBS (red; simulating a fasted state and known as FaSSIF V1, [5]), and in TC/L at fivefold concentration in PBS as compared to FaSSIF V1 (purple; simulating a fed state and known as FeSSIF V1[5]). Flux was significantly reduced for Perphenazine and Imatinib in TC/L in PBS and in 5xTC/L in PBS. Metoprolol flux was not significantly reduced in TC/L in PBS compared to PBS, but in 5xTC/L in PBS. Data shown as mean ± SD, ANOVA considering $p \leq 0.05$ as statistically significant followed by Games-howell <i>post-hoc</i> test for pairwise comparison as the criteria of variance homogeneity was not fulfilled (significant differences are shown by asterisks).	34
Figure S37: Flux of (A) Perphenazine, (B) Imatinib, and (C) Metoprolol at different starting concentrations (100, 250, 500, and 1000 μmol/l) in PBS (black) and in TC/L in PBS (red). Flux increased linearly over concentration in all cases in TC/L in PBS. In PBS at 1000 μM flux for (A) Perphenazine and (B) Imatinib did not follow the linear trend of measurements at low concentrations (data point in brackets). Nevertheless, flux was stable over time for this concentration (Figure S37). Data shown as a single point measurement.	35
Figure S38: (A) Perphenazine, (B) Imatinib, and (C) Metoprolol concentration [μmol/l] in the flux acceptor compartment in PBS (black), in TC/L in PBS (simulating fasted state/FaSSIF V1; red), and	

with TC/L at fivefold concentration in PBS as compared to FaSSIF V1 (simulating fed state; FeSSIF V1; purple) over time at a starting concentration of 1000 $\mu\text{mol/l}$ in the donor compartment. Concentration increased linearly over time in all cases indicating stable experimental conditions. Data shown as mean \pm SD. 36

Figure S39: Perphenazine concentration [$\mu\text{mol/l}$] in the flux acceptor compartment over time with (A, B) Colesevelam, (C, D) Eudragit E, (E, F) Soluplus in TC/L in PBS (respective left panel) and in PBS (respective right panel) at concentrations as indicated. Data at 0% polymer concentration are identical for all panels and given for comparison. 37

Figure S40: Perphenazine concentration [$\mu\text{mol/l}$] in the flux acceptor compartment over time with (A, B) Kollidon VA 64, (C, D) HPMCAS in TC/L in PBS (respective left panel) and in PBS (respective right panel) at concentrations as indicated. Data at 0% polymer concentration are identical for all panels and given for comparison. 38

Figure S41: Imatinib concentration [$\mu\text{mol/l}$] in the flux acceptor compartment over time with (A, B) Colesevelam, (C, D) Eudragit E, (E, F) Soluplus in TC/L in PBS (respective left panel) and in PBS (respective right panel) at concentrations as indicated. Data at 0% polymer concentration are identical for all panels and given for comparison. 39

Figure S42: Imatinib concentration [$\mu\text{mol/l}$] in the flux acceptor compartment over time with (A, B) Kollidon VA 64, (C, D) HPMCAS in TC/L in PBS (respective left panel) and in PBS (respective right panel) at concentrations as indicated. Data at 0% polymer concentration are identical for all panels and given for comparison. 40

Figure S43: Metoprolol concentration [$\mu\text{mol/l}$] in the flux acceptor compartment over time with polymers as indicated (A) in TC/L in PBS and (B) in PBS at 1% polymer concentration. Data at 0% polymer concentration are provided in each panel. 41

Figure S44: Lag time of Perphenazine with (A) Colesevelam, (B) Eudragit E, (C) Soluplus, (D) Kollidon VA 64, and (E) HPMC-AS in TC/L in PBS (red) and in PBS (black) at concentrations as indicated. The data reported at 0% are identical for all panels and given for comparison. Data for (B) Eudragit E is also shown in Figure 6 in the manuscript. Lag time was calculated by time axis intersect of the extrapolated linear part (**Figure S36**). Data shown as mean \pm SD, ANOVA considering $p \leq 0.05$ as statistically significant followed by Tukey post-hoc test for pairwise comparison (significant differences are shown by asterisks). 43

Figure S45: Lag time of Imatinib with (A) Colesevelam, (B) Eudragit E, (C) Soluplus, (D) Kollidon VA 64, and (E) HPMC-AS in TC/L in PBS (red) and in PBS (black) at concentrations as indicated. The first bars 0% are identical for all panels and for comparison. Data for (B) Eudragit E is also shown in Figure 6 in the manuscript. Lag time was calculated by time axis intersect of linear concentration over time extrapolation (**Figure S36**). Data shown as mean \pm SD, ANOVA considering $p \leq 0.05$ as statistically significant followed by Tukey post-hoc test for pairwise comparison (significant differences are shown by asterisks). 45

Figure S46: Metoprolol lag time (0) in absence of polymer, with 1% (A) Colesevelam, (B) Eudragit E, (C) Soluplus, (D) Kollidon VA 64, and (E) HPMC-AS in TC/L in PBS (red) and in PBS (black). No difference in lag time between the groups was observed. 46

Tables:

Table S1: Polymer dynamic viscosities in TC/L in PBS and in PBS at 25 °C used for DLS data adjustment [$\text{mPa}\cdot\text{s}$]. 12

Table S2: Mean polydispersity index (PDI) with standard deviation of colloids in TC/L in PBS. 12

Table S3: Mean polydispersity index (PDI) with standard deviation of colloids in PBS. 13

Table S4: HDO diffusion coefficients (D in m^2/s) for polymers in TC/L in PBS with Perphenazine at 4.703 ppm. 32

Table S5: Perphenazine aryl-proton diffusion coefficients (D in m^2/s) for polymers (0.05%) in TC/L in PBS at 7.2 and 6.7 ppm. Preliminary data set as signal decay did not reach $< 10\%$ of initial intensity. 32

Table S6: Double-sided Grubb's outlier test for lag time of Perphenazine in PBS, in TC/L in PBS, in TC/L in PBS with 1% Eudragit E, and in TC/L in PBS with 1% HPMC-AS with a significance level of 0.05. One outcome was excluded as highlighted in bold/italic numbers. 42

Table S7: double-sided Grubb's outlier test for lag time of Imatinib in TC/L in PBS, in TC/L in PBS with 1% Eudragit E, in TC/L in PBS with 1% Soluplus, and in TC/L in PBS with 1% HPMC-AS with a significance level of 0.05. One outcome was excluded as highlighted in bold/italic numbers. 44

S1 Methods

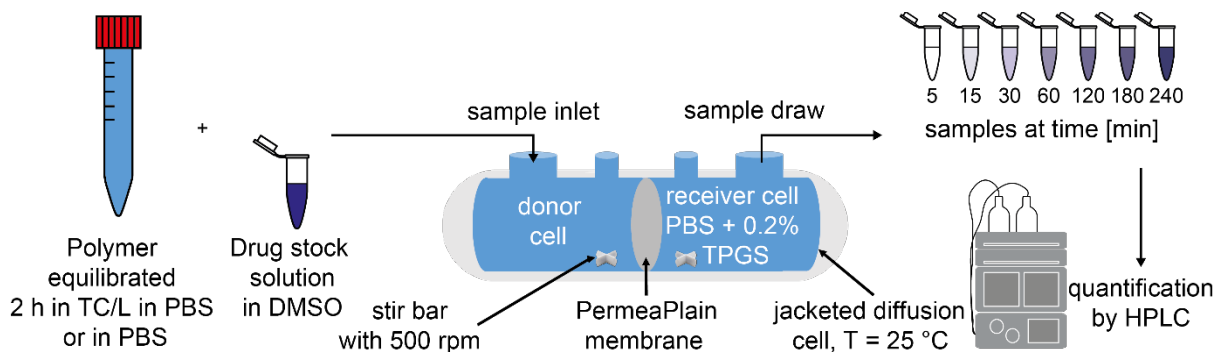
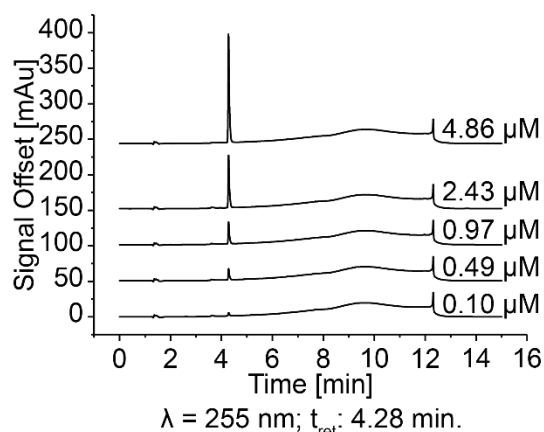
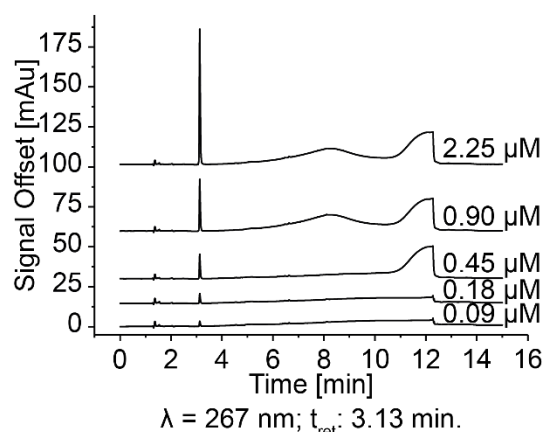


Figure S1: Flux assay as described in 2.2.3

A Perphenazine



B Imatinib



C Metoprolol

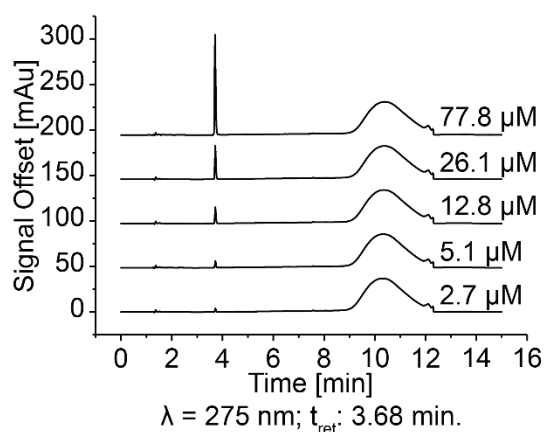


Figure S2: HPLC calibration spectra for (A) Perphenazine, (B) Imatinib, and (C) Metoprolol. Signal area under the curve (AUC) increased linearly with concentration. Respective nominal drug concentrations are shown on the right side of each spectrum. λ represents wavelength of detector and t_{ret} retention time of respective drug peak.

S2 ¹H nuclear magnetic resonance (NMR) data interpretation

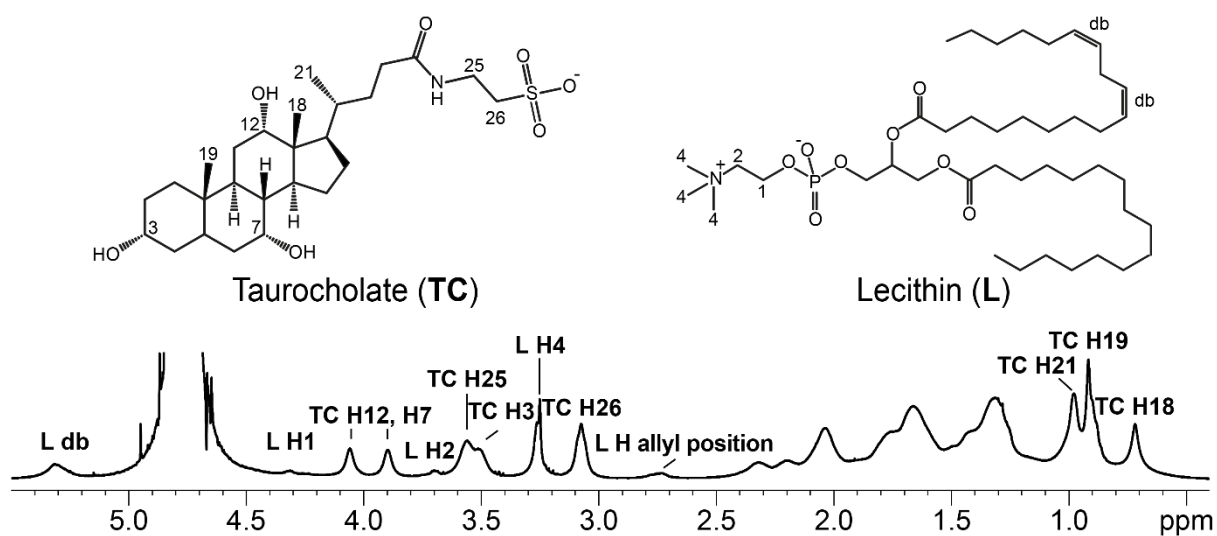


Figure S3: ¹H NMR signal assignment of taurocholate (TC) and lecithin (L) based on [1].

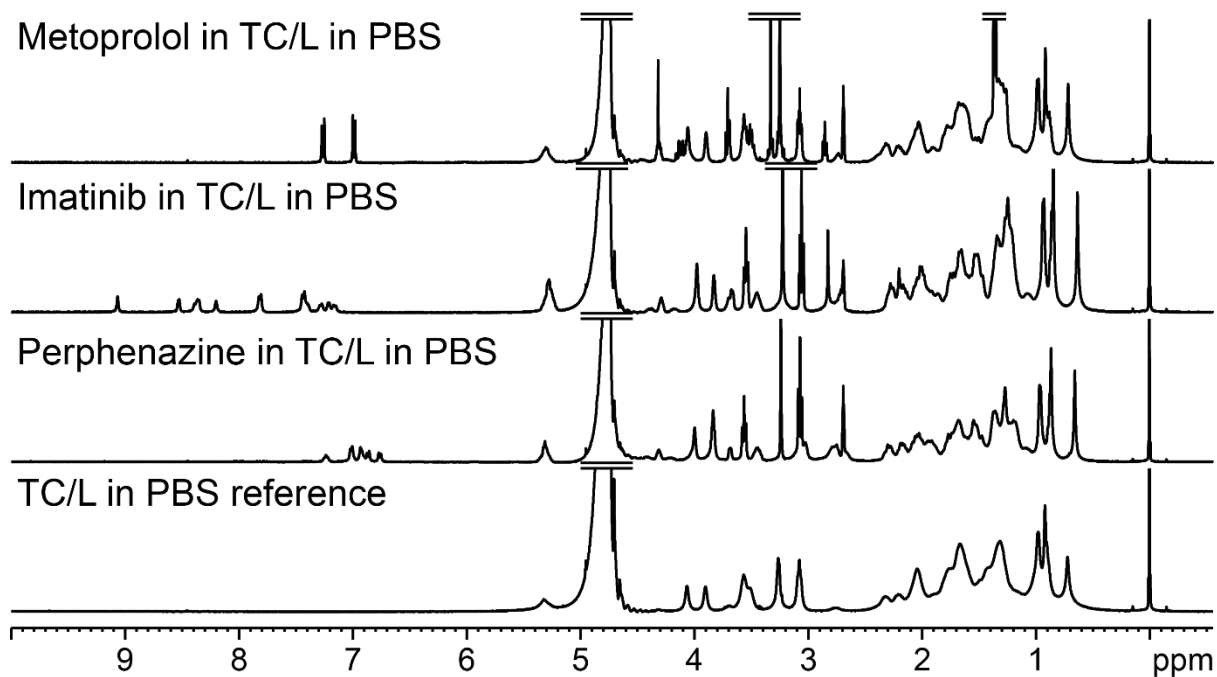
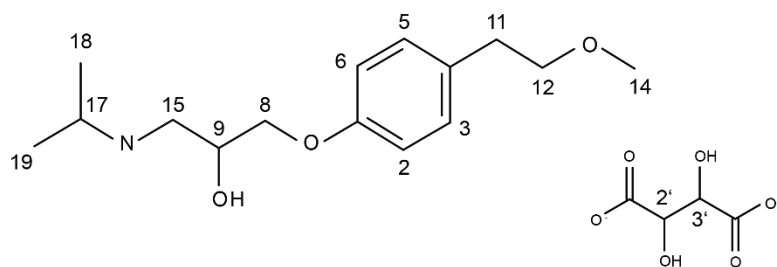
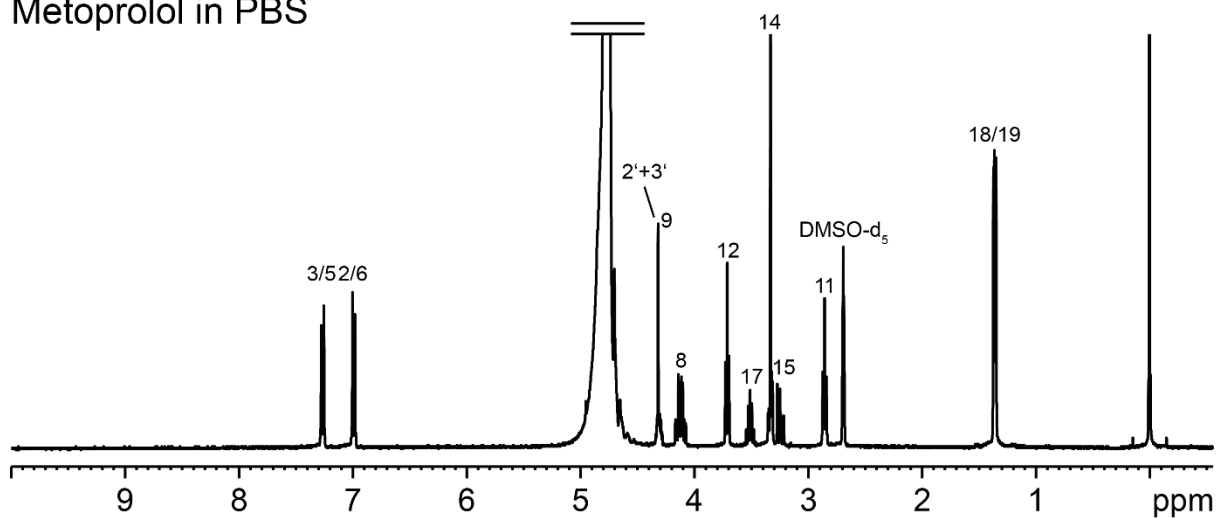


Figure S4: Complete ¹H NMR spectra of Metoprolol, Imatinib, and Perphenazine with TC/L. Bottom shows TC/L reference spectrum.

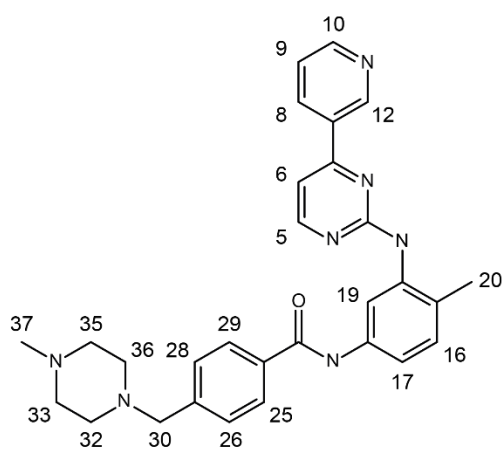
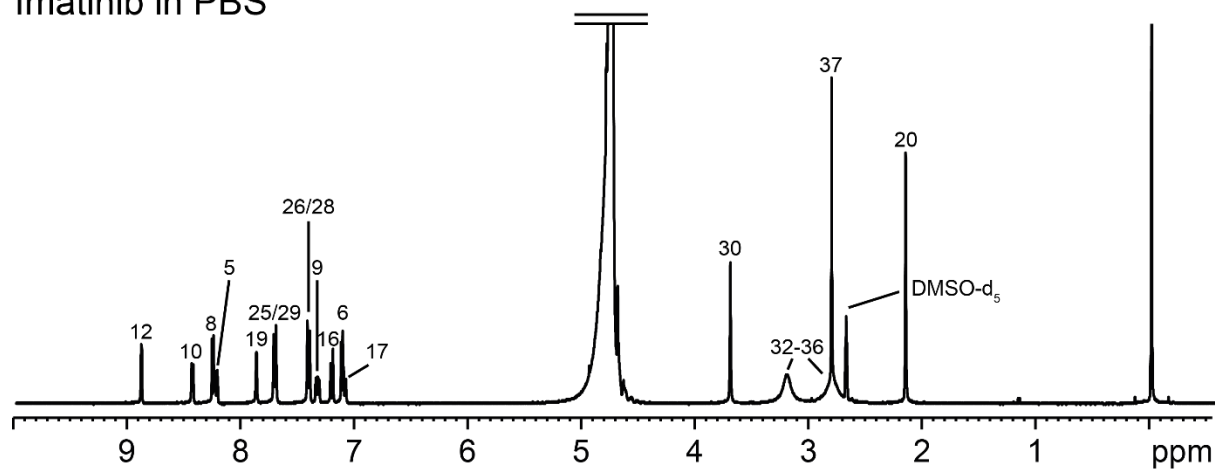
Metoprolol in PBS



Metoprolol (tartrate)

Figure S5: Complete ^1H NMR spectrum with signal assignment and respective molecular structure of Metoprolol in PBS. Standard 1D and 2D NMR techniques were applied for signal assignment.

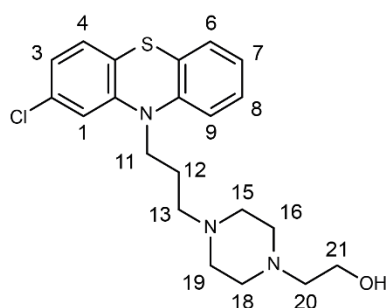
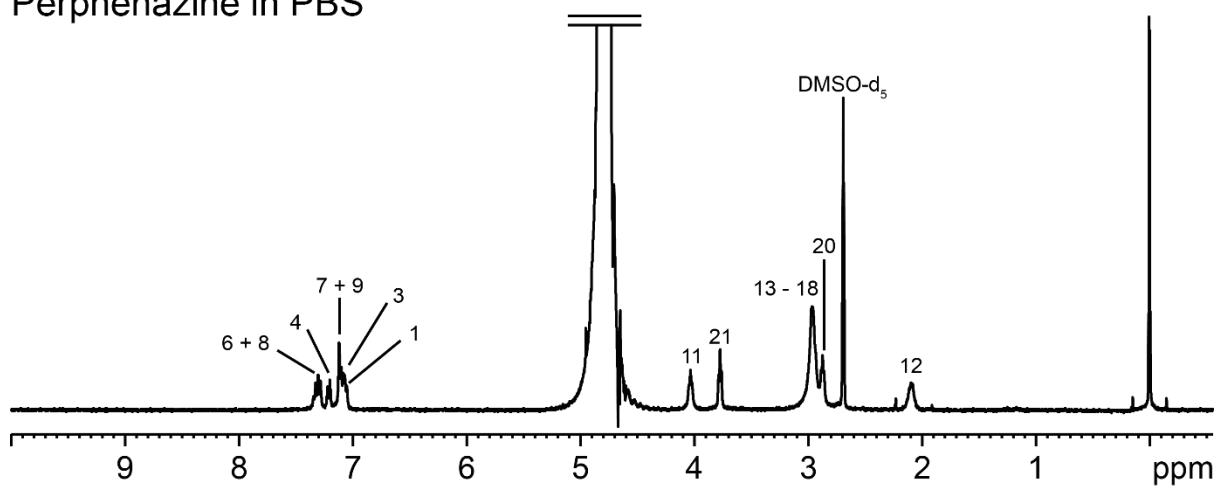
Imatinib in PBS



Imatinib

Figure S6: Complete ^1H NMR spectrum with signal assignment and respective molecular structure of Imatinib in PBS. Standard 1D and 2D NMR techniques were applied for signal assignment.

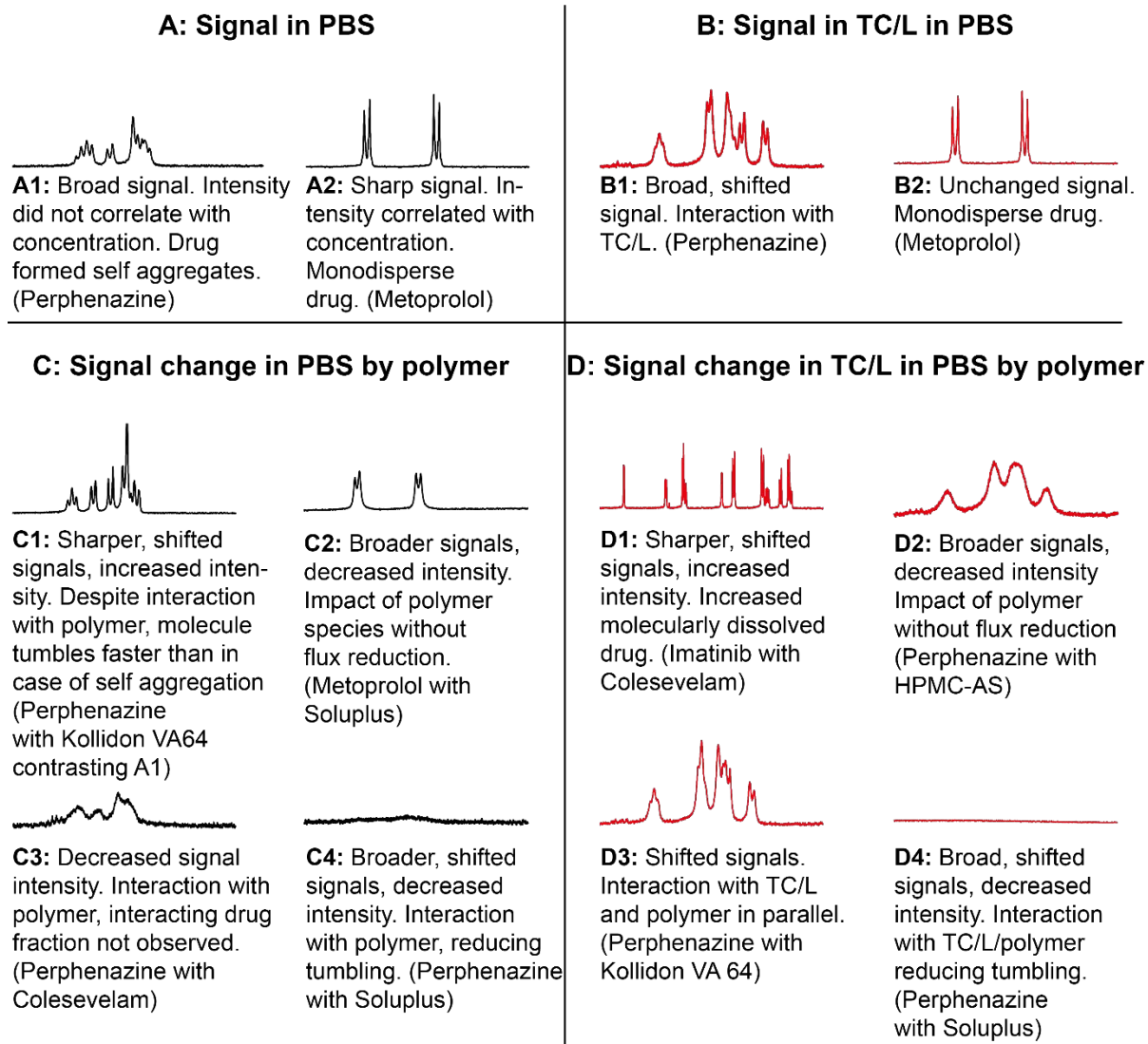
Perphenazine in PBS



Perphenazine

Figure S7: Complete ^1H NMR spectrum with signal assignment and respective molecular structure of Perphenazine in PBS. Standard 1D and 2D NMR techniques were applied for signal assignment.

Analysis of drug aryl-proton signal



Note: A low molecular tumbling (shorter T_2 relaxation time) indicates a possible interaction with supramolecular aggregates, but interaction can also increase molecular tumbling (Kollidon VA 64). Therefore, tumbling rate does not necessarily reflect amount of molecularly dissolved drug. Perphenazine and Imatinib self-aggregate in PBS, therefore signal integrals were not analyzed

Figure S8: Interpretation of the NMR spectral patterns of the aryl-proton signals of drug molecules without polymer in PBS (A) and in TC/L in PBS (B) and with polymer in PBS (C) and in TC/L in PBS (D).

S3 Polymer characterization in TC/L in PBS and in PBS

S3.1 Particle size analysis in PBS by dynamic light scattering (DLS)

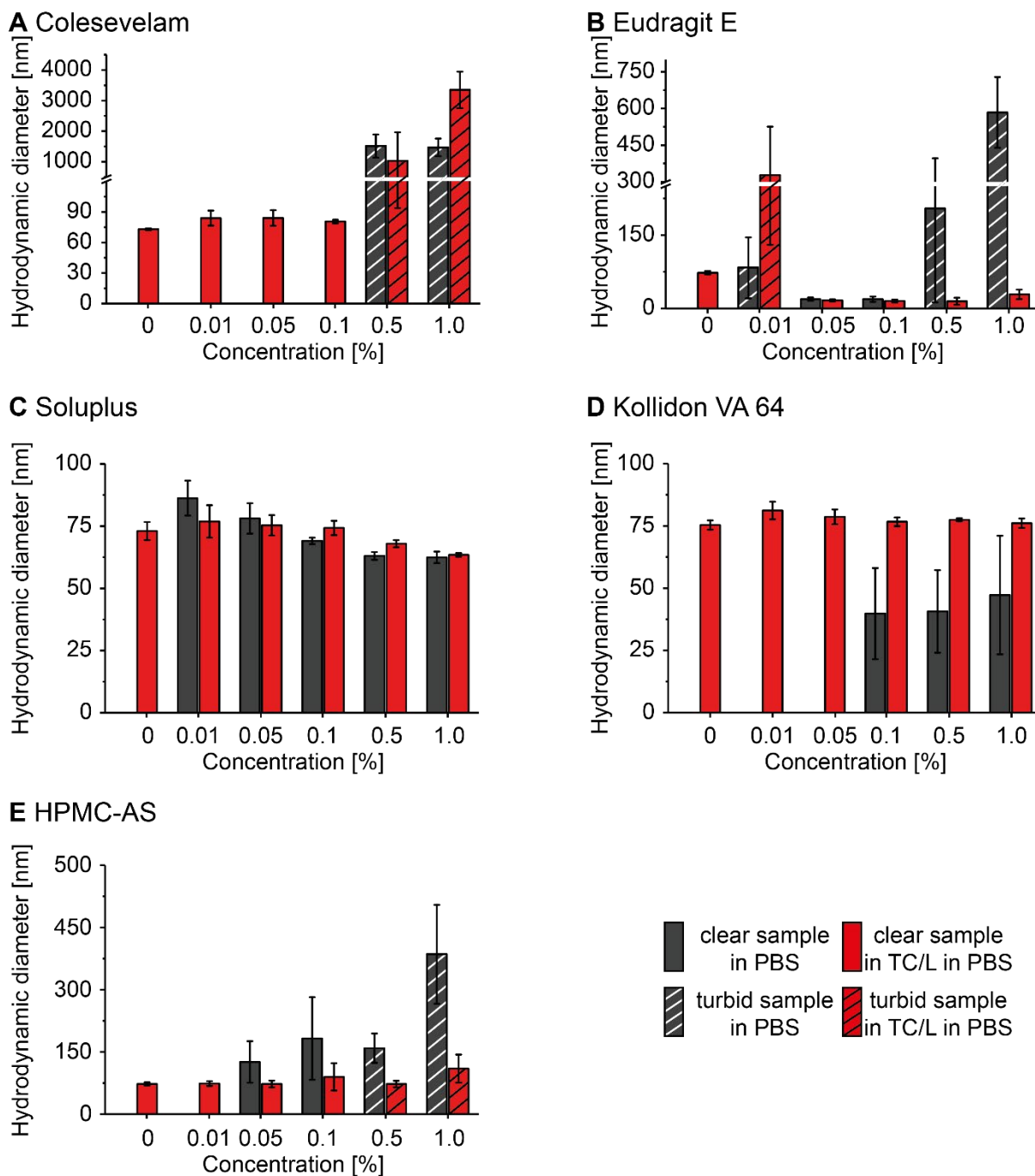


Figure S9: Mean hydrodynamic diameters of colloids in PBS (grey) and in TC/L in PBS (red) with (A) Colesevelam, (B) Eudragit E, (C) Soluplus, (D) Kollidon VA 64, and (E) HPMC-AS at different concentrations by DLS (mean \pm SD). At $\geq 0.5\%$ Colesevelam particles were detected (A grey). Turbidity was also observed for Eudragit E at 0.01, 0.5, and 1% (B, grey). At 0.05 and 0.1% Eudragit E formed colloids around 20 nm. Conversely, Eudragit E in TC/L in PBS formed colloids at $\geq 0.05\%$ (B, red). Soluplus formed 60-90 nm particles in PBS (C, grey). At $\geq 0.1\%$ Kollidon VA 64 particles around 40 nm were observed (D, grey). Hydrodynamic diameters of HPMC-AS ranged from 70 to 250 nm at 0.05 and 0.1% (E, grey). At $\geq 0.5\%$ particle size up to 500 nm were observed along with turbidity.

Table S1: Polymer dynamic viscosities in TC/L in PBS and in PBS at 25 °C used for DLS data adjustment [mPa*s].

Concentration [%]	Colesevelam		Eudragit E		Soluplus		Kollidon VA 64		HPMC-AS	
	PBS	TC/L in PBS	PBS	TC/L in PBS	PBS	TC/L in PBS	PBS	TC/L in PBS	PBS	TC/L in PBS
0.01			0.9410	0.9457	0.9431	0.9312	N/A	0.9339	N/A	0.9488
0.05			0.9300	0.9258	0.9255	0.9400	N/A	0.9398	0.9540	0.9767
0.1	N/A	N/A	0.9337	0.9275	0.9269	0.9450	0.9527	0.9503	1.0014	1.0251
0.5			0.9689	0.9422	0.9572	0.9805	0.9866	1.0116	1.3985	1.3942
1			0.9366	0.9602	1.0014	1.0376	1.0685	1.0945	1.8190	1.4707
PBS						0.9104				
TC/L reference						0.9258				

Table S2: Mean polydispersity index (PDI) with standard deviation of colloids in TC/L in PBS.

Concentration [%]	Colesevelam		Eudragit E		Soluplus		Kollidon VA 64		HPMC-AS	
	PDI mean	PDI SD	PDI mean	PDI SD	PDI mean	PDI SD	PDI mean	PDI SD	PDI mean	PDI SD
0.01	0.075	0.036	0.23	0.12	0.108	0.007	0.143	0.032	0.083	0.049
0.05	0.050	0.030	0.180	0.088	0.099	0.018	0.086	0.020	0.060	0.015
0.1	0.095	0.015	0.19	0.10	0.077	0.033	0.097	0.012	0.107	0.078
0.5	0.40	0.24	0.13	0.13	0.066	0.024	0.104	0.032	0.126	0.044
1	0.933	0.070	0.249	0.029	0.062	0.013	0.127	0.025	0.173	0.014
TC/L reference	0.144	0.057	0.06	0.030	0.056	0.041	0.069	0.019	0.06	0.030

Table S3: Mean polydispersity index (PDI) with standard deviation of colloids in PBS.

Concentration [%]	Colesevelam		Eudragit E		Soluplus		Kollidon VA 64		HPMC-AS	
	PDI mean	PDI SD	PDI mean	PDI SD	PDI mean	PDI SD	PDI mean	PDI SD	PDI mean	PDI SD
0.01	N/A	N/A	0.32	0.26	0.14	0.02	N/A	N/A	N/A	N/A
0.05	N/A	N/A	0.20	0.13	0.088	0.023	N/A	N/A	0.30	0.09
0.1	N/A	N/A	0.27	0.01	0.059	0.013	0.40	0.03	0.21	0.07
0.5	0.52	0.15	0.23	0.08	0.051	0.018	0.24	0.04	0.23	0.03
1	0.37	0.09	0.30	0.04	0.053	0.024	0.23	0.02	0.36	0.03

S3.2 ^1H nuclear magnetic resonance (^1H NMR) analysis of polymers

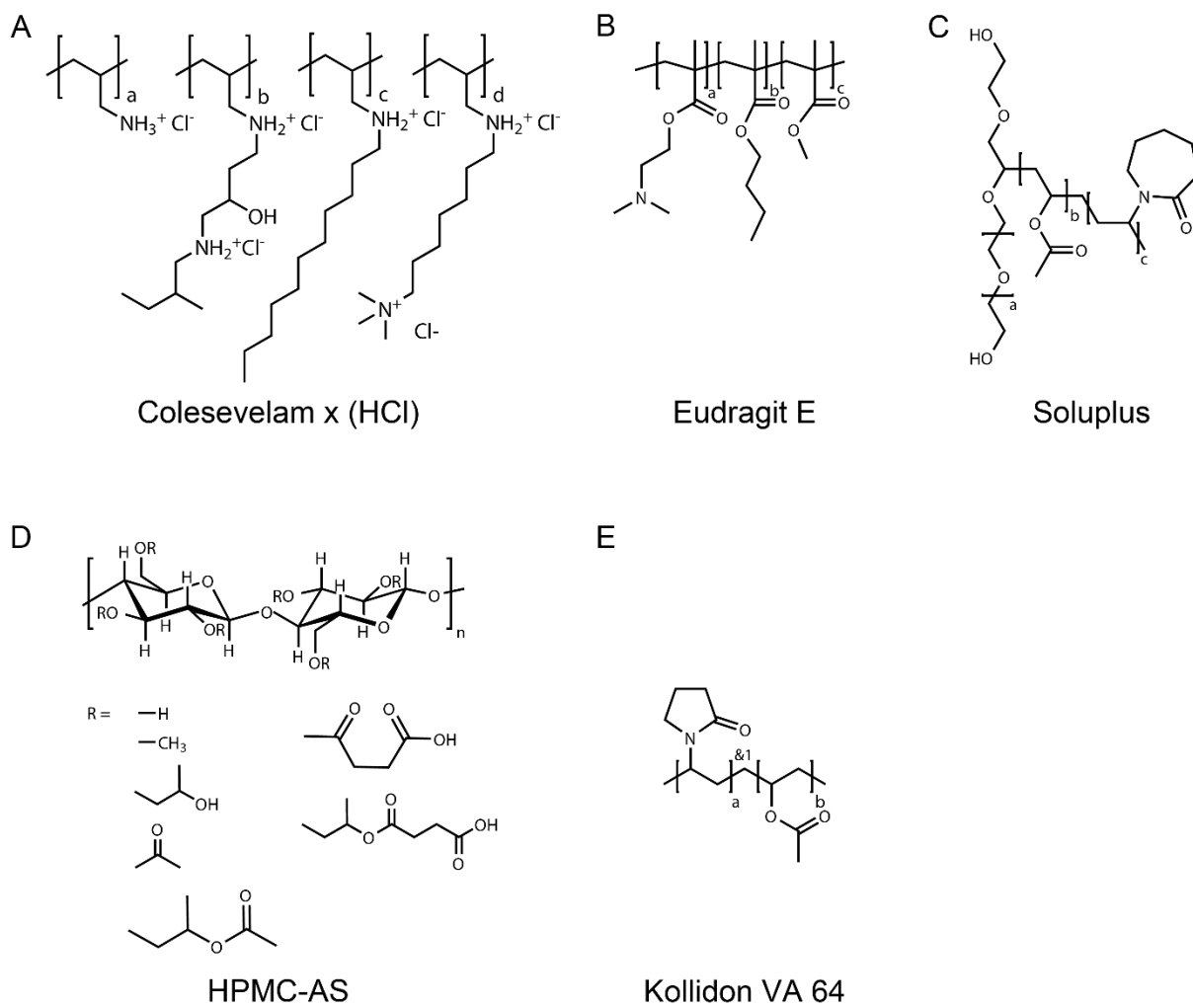


Figure S10: Chemical structures of used polymers.

S3.2.1 Colesevelam in PBS

Colesevelam in PBS

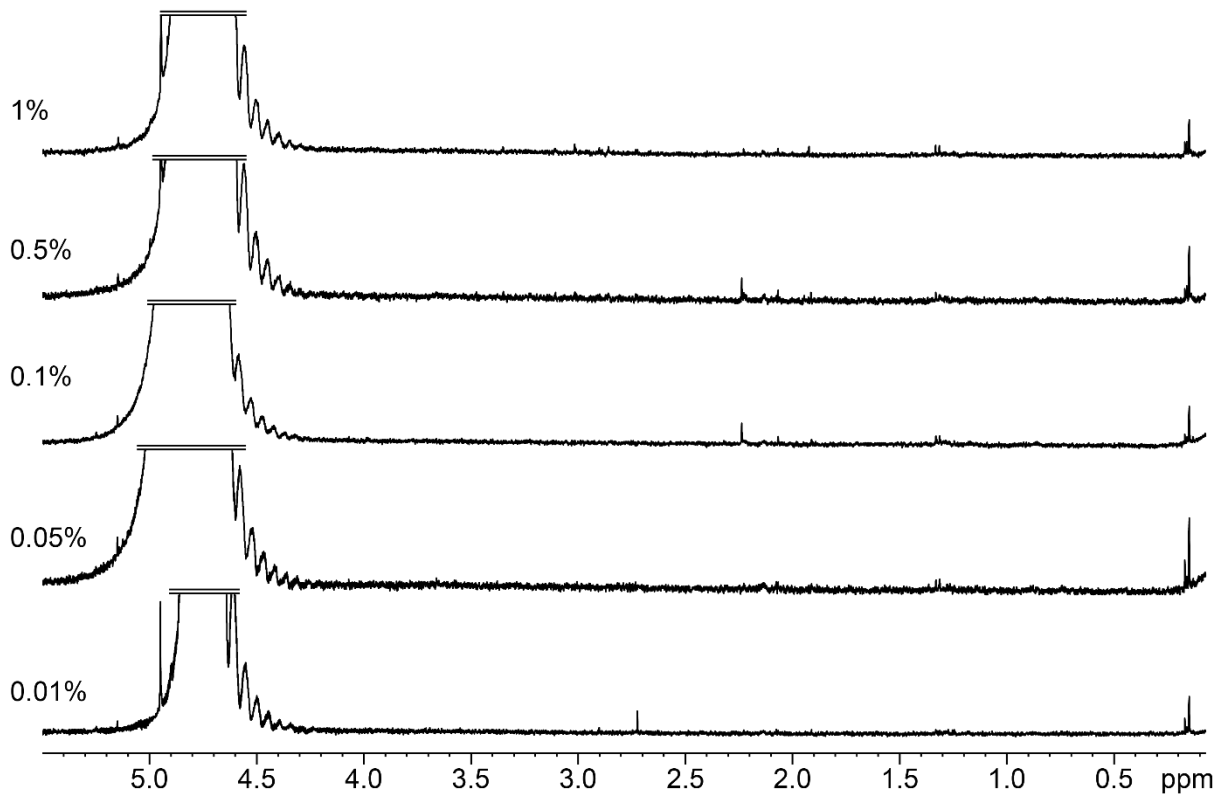


Figure S11: ¹H NMR spectra of Colesevelam at 0.01, 0.05, 0.1, 0.5, and 1% in PBS. No Colesevelam signals were detected.

S3.2.2 Colesevelam in TC/L in PBS

Colesevelam in TC/L in PBS

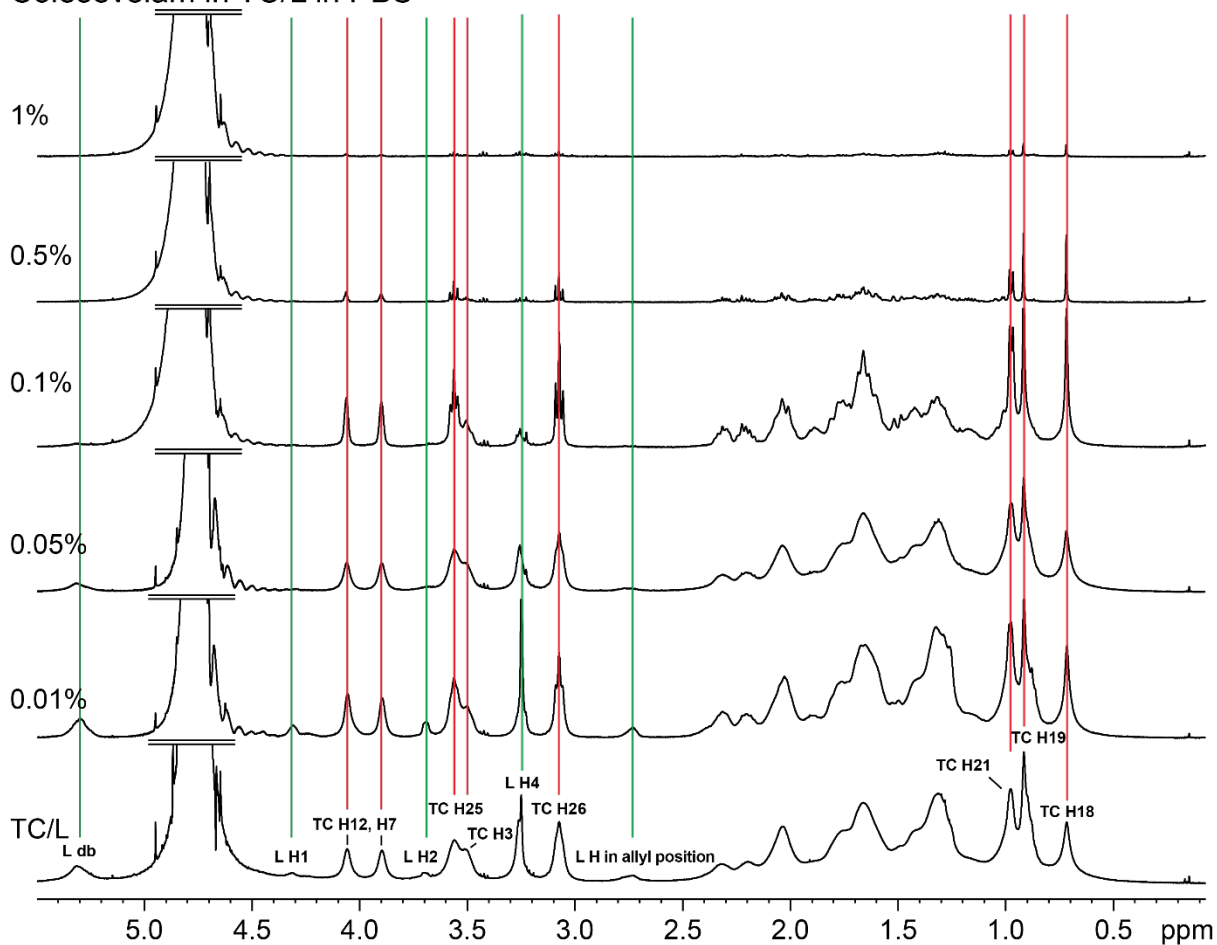


Figure S12: ¹H NMR spectra of Colesevelam at 0.01, 0.05, 0.1, 0.5, and 1% in TC/L in PBS indicated as (L) green lines and (TC) red lines. TC/L reference spectrum is shown (bottom). TC/L signal intensities decreased as a function of Colesevelam concentration. At $\geq 0.1\%$ signals sharpened (e.g. TC H25 and H26). At $\geq 0.5\%$ sharp TC signals with low intensity were found indicating precipitation of TC/L. Few TC remains in solution, but does not aggregate.

S3.2.3 Eudragit E in PBS

Eudragit E in PBS

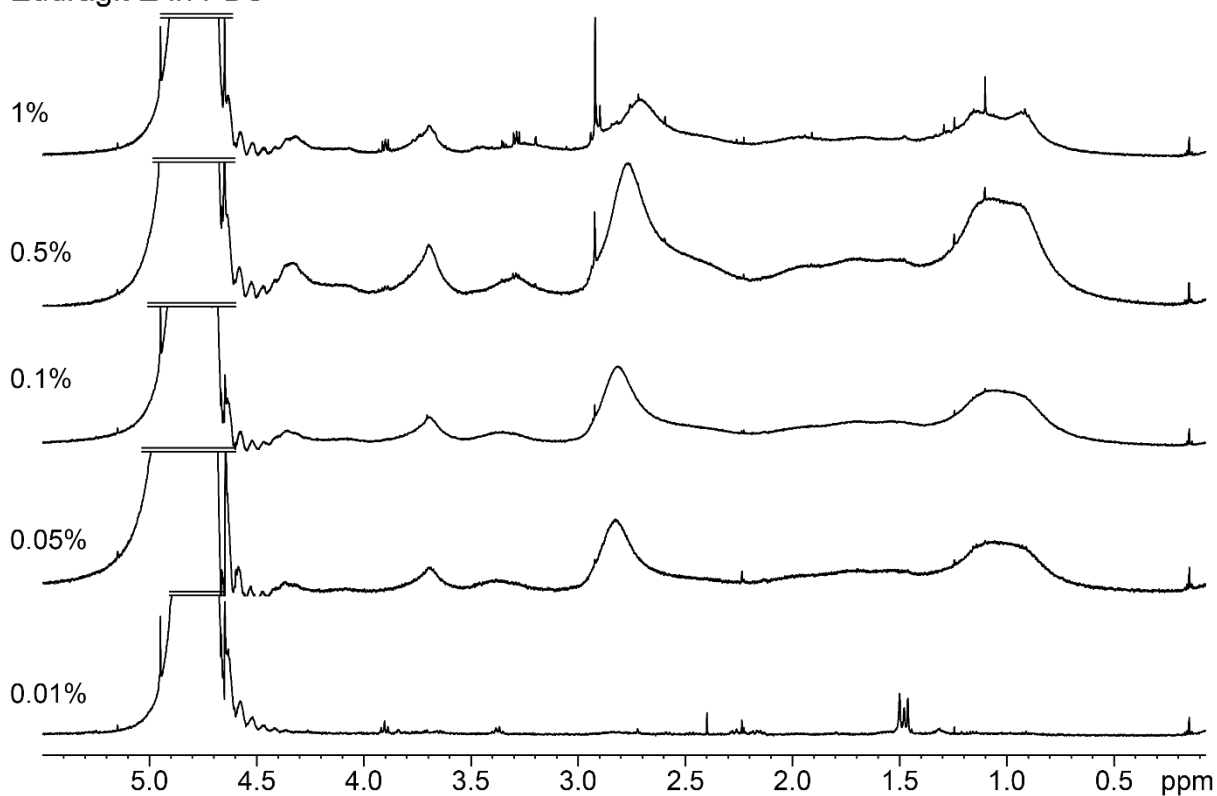


Figure S13: ¹H NMR spectra of Eudragit E at 0.01, 0.05, 0.1, 0.5, and 1% in PBS. Sharp signals with low intensity were detected at 0.01%. At $\geq 0.05\%$, broad Eudragit E signals were observed. Some sharp signals shifted to lower ppm dependent on concentration (e.g. at 2.8 ppm).

S3.2.4 Eudragit E in TC/L in PBS

Eudragit E in TC/L in PBS

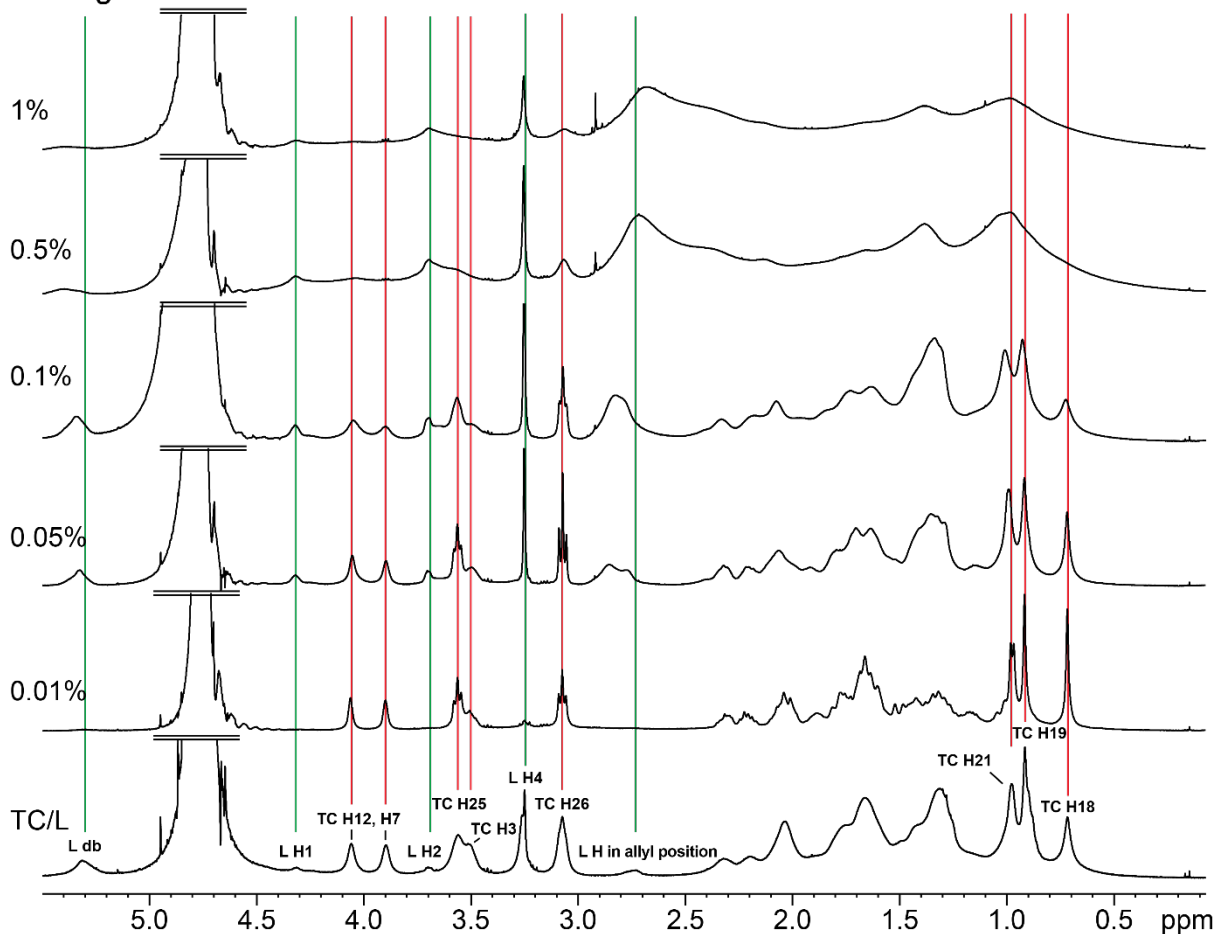


Figure S14: ^1H NMR spectra of Eudragit E at 0.01, 0.05, 0.1, 0.5, and 1% in TC/L in PBS indicated as (L) green lines and (TC) red lines. TC/L reference spectrum is shown (bottom). At 0.01% L signals disappeared, while TC signals sharpened. At $\geq 0.05\%$ L signals reappeared. At $\geq 0.1\%$ some TC/L signals shifted and at $\geq 0.5\%$ disappeared (e.g. TC H21, H19, and 18). Other signals did not disappear, but intensity decreased along with signal broadening (e.g. L H4, TC H26).

S3.2.5 Soluplus in PBS

Soluplus in PBS

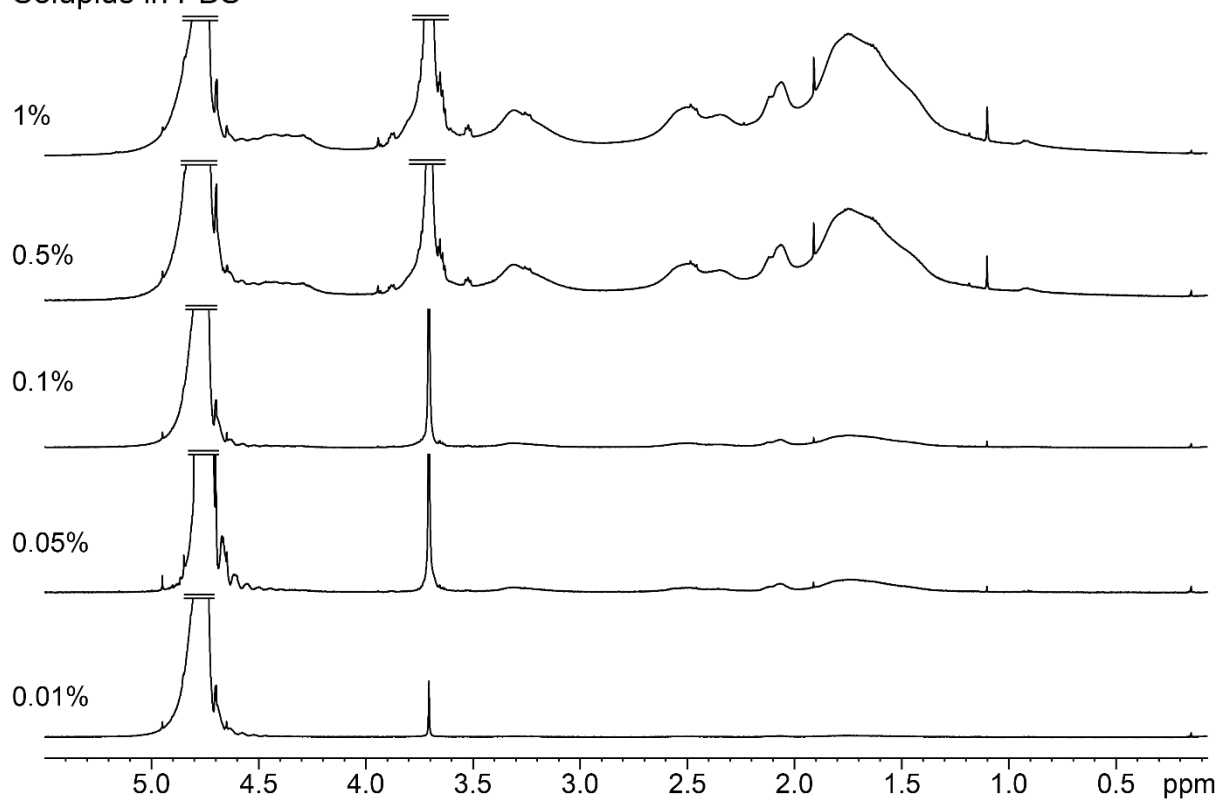


Figure S15: ¹H NMR spectra of Soluplus at 0.01, 0.05, 0.1, 0.5 and 1% in PBS. Signal intensity increased as a function of concentration. Broad signals (e.g. at 1.3-2.6 ppm) and sharp signals (e.g. at 1.1 and 1.9 ppm) were detected in parallel.

S3.2.6 Soluplus in TC/L in PBS

Soluplus in TC/L in PBS

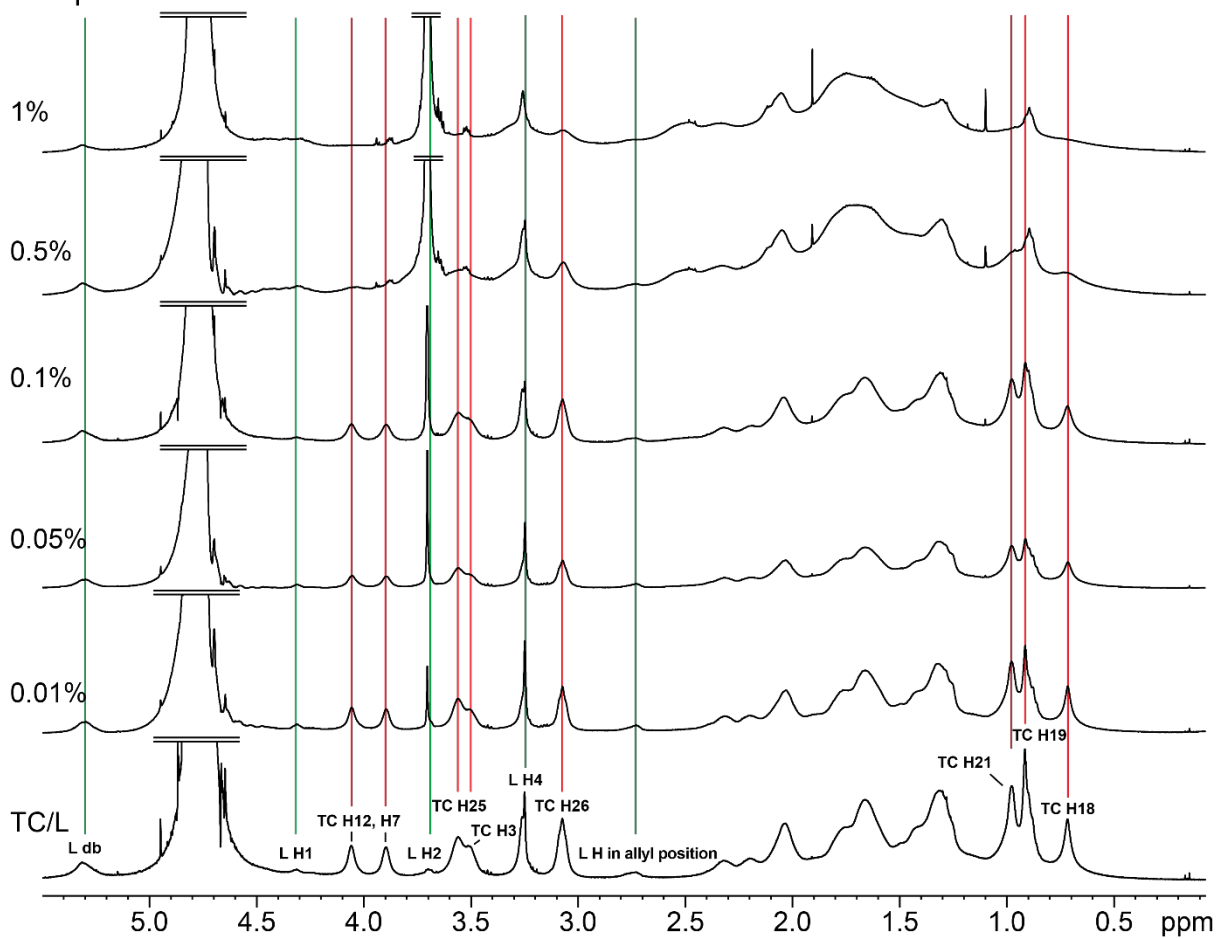


Figure S16: ¹H NMR spectra of Soluplus at 0.01, 0.05, 0.1, 0.5 and 1% in TC/L in PBS indicated as (L) green lines and (TC) red lines. TC/L reference spectrum is shown (bottom). At 1% some TC signals appeared very broad (e.g. TC H12, H7, H25, H3, H21, H19, and H18). Other signals were still observed (e.g. all L and TC H26).

S3.2.7 Kollidon VA 64 in PBS

Kollidon VA 64 in PBS

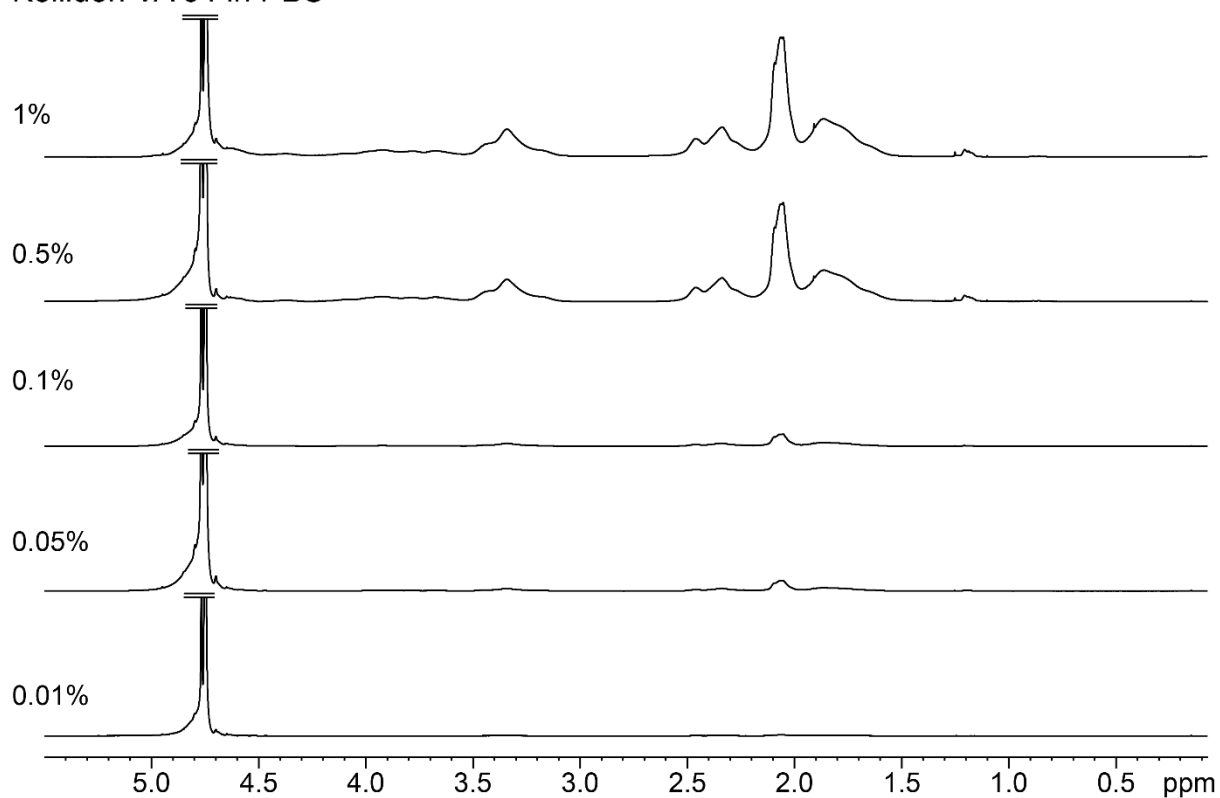


Figure S17: ¹H NMR spectra of Kollidon VA 64 at 0.01, 0.05, 0.1, 0.5 and 1% in PBS. Signal intensity increased as a function of concentration. Broad signals (e.g. at 1.6-2.5 ppm) were detected.

S3.2.8 Kollidon VA 64 in TC/L in PBS

Kollidon VA 64 in TC/L in PBS

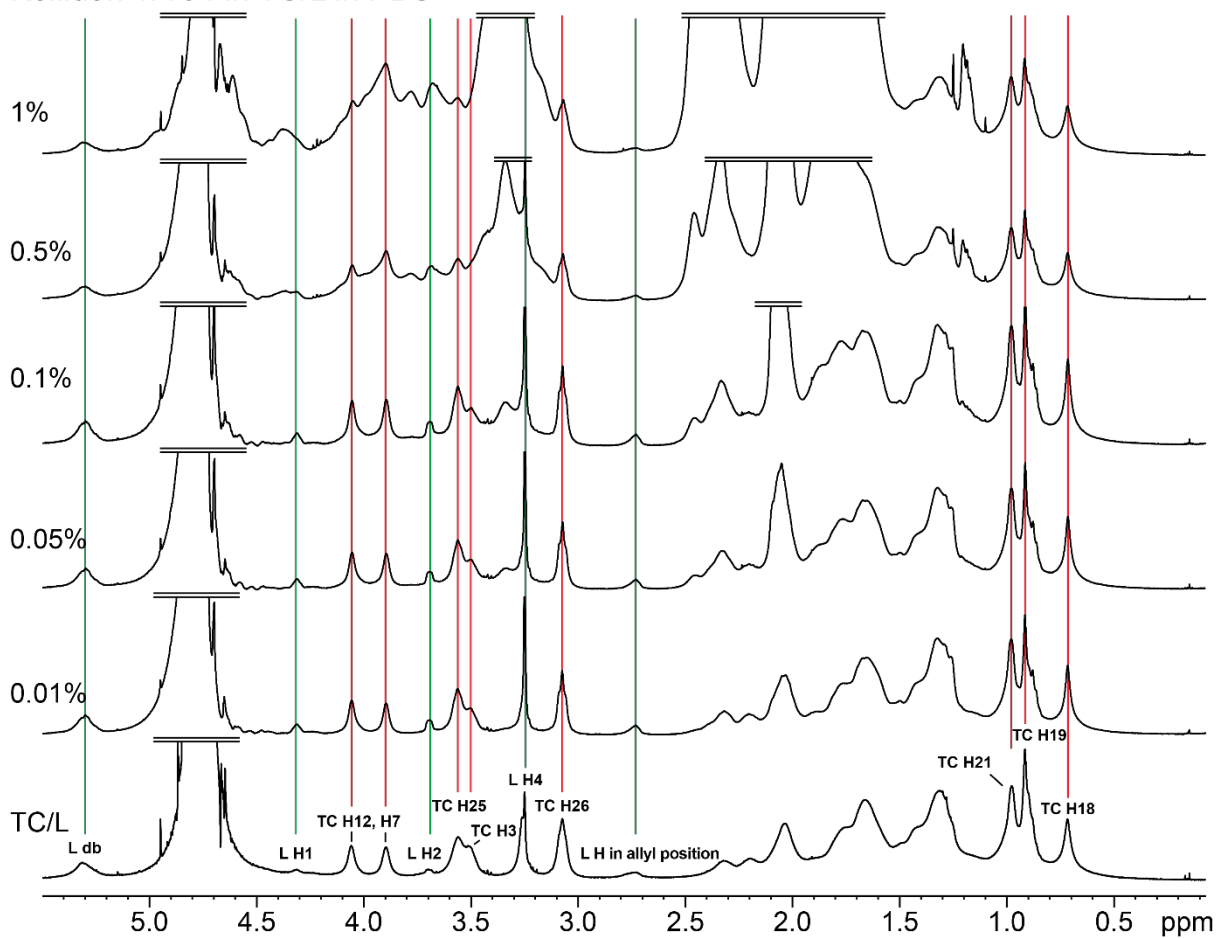


Figure S18: ^1H NMR spectra of Kollidon VA 64 at 0.01, 0.05, 0.1, 0.5 and 1% in TC/L in PBS indicated as (L) green lines and (TC) red lines. TC/L reference spectrum is shown (bottom). TC/L signals did not change. Kollidon VA 64 signals increased as a function of concentration overlapping with TC/L signals.

S3.2.9 HPMC-AS in PBS

HPMC-AS in PBS

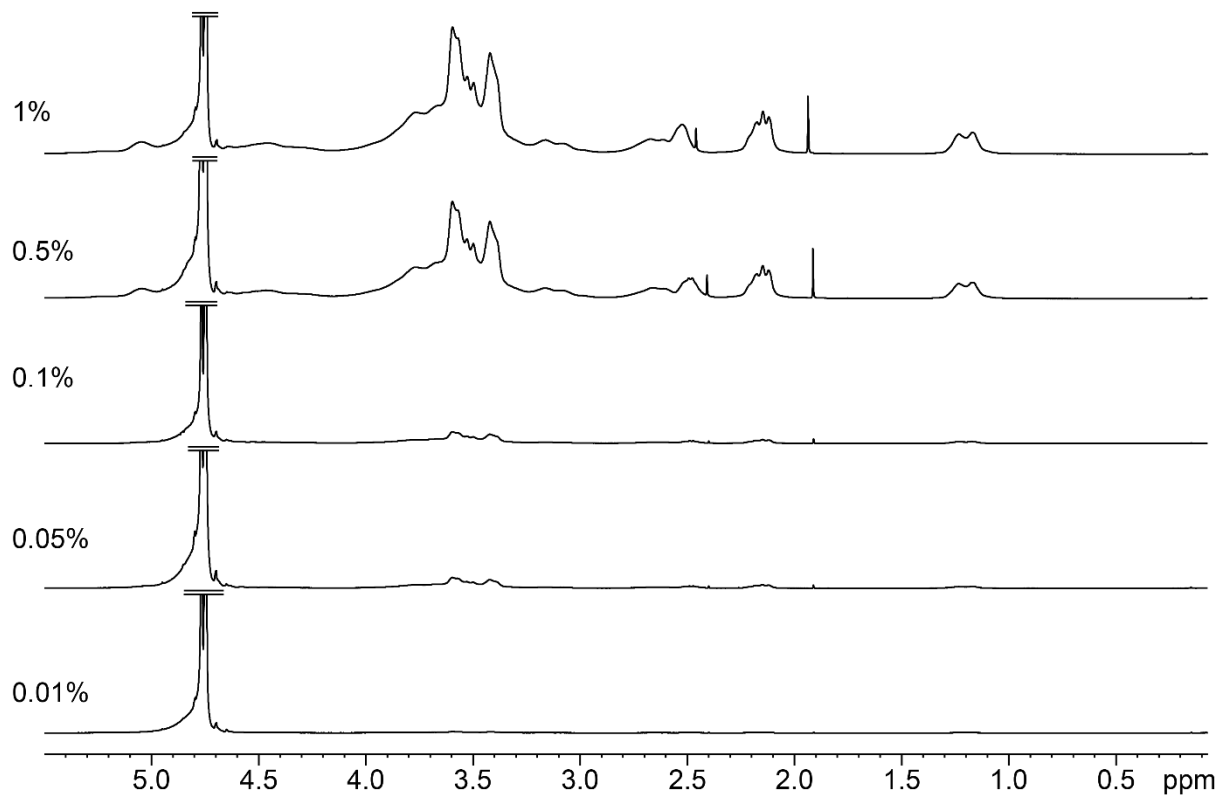
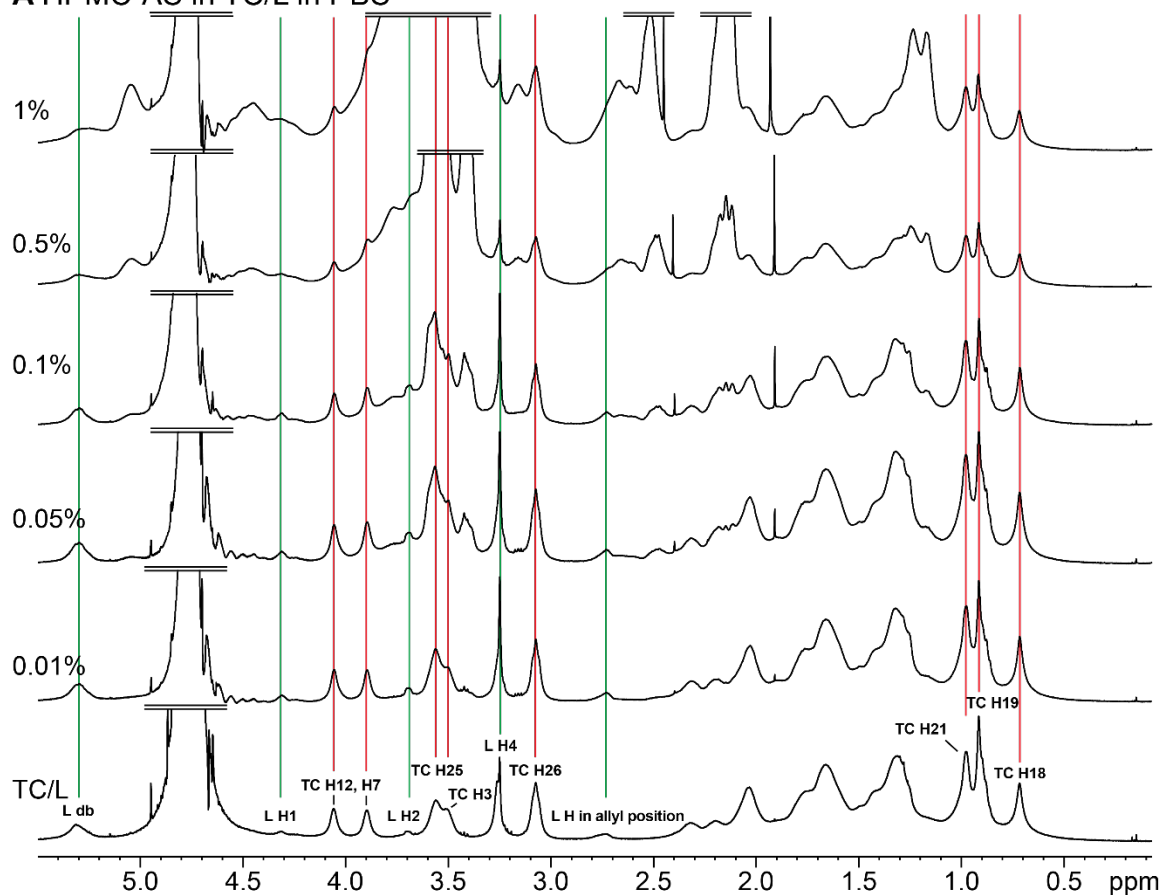


Figure S19: ¹H NMR spectra of HPMC-AS at 0.01, 0.05, 0.1, 0.5 and 1% in PBS. Signal intensity increased as a function of concentration. Broad signals (e.g. at 3.0-4.0 ppm) were detected along with sharp signals (e.g. at 1.9 and 2.4 ppm).

S3.2.10 HPMC-AS in TC/L in PBS

A HPMC-AS in TC/L in PBS



B

1% HPMC-AS in TC/L in PBS
TC/L in PBS no polymer

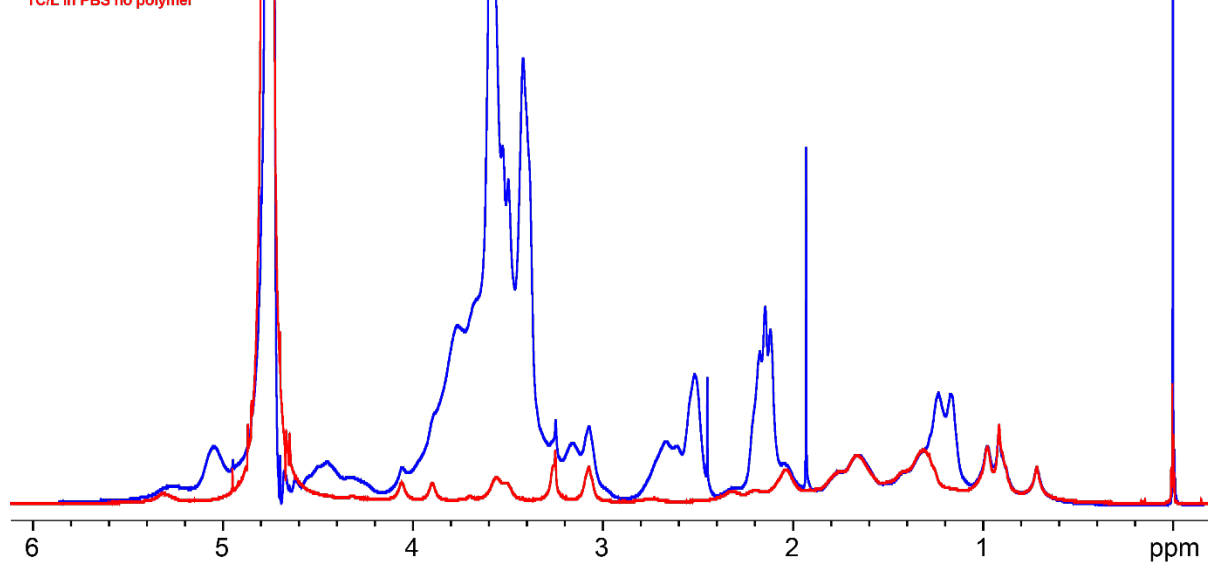


Figure S20: (A) ^1H NMR spectra of HPMC-AS at 0.01, 0.05, 0.1, 0.5 and 1% in TC/L in PBS indicated as (L) green lines and (TC) red lines. TC/L reference spectrum is shown (bottom). (B) Overlay of 1% HPMC-AS with TC/L and TC/L reference spectrum (B). TC/L signals did not change. HPMC-AS signals increased as a function of concentration and overlapped TC/L signals.

S3.2.11 Complete ^1H NMR spectra

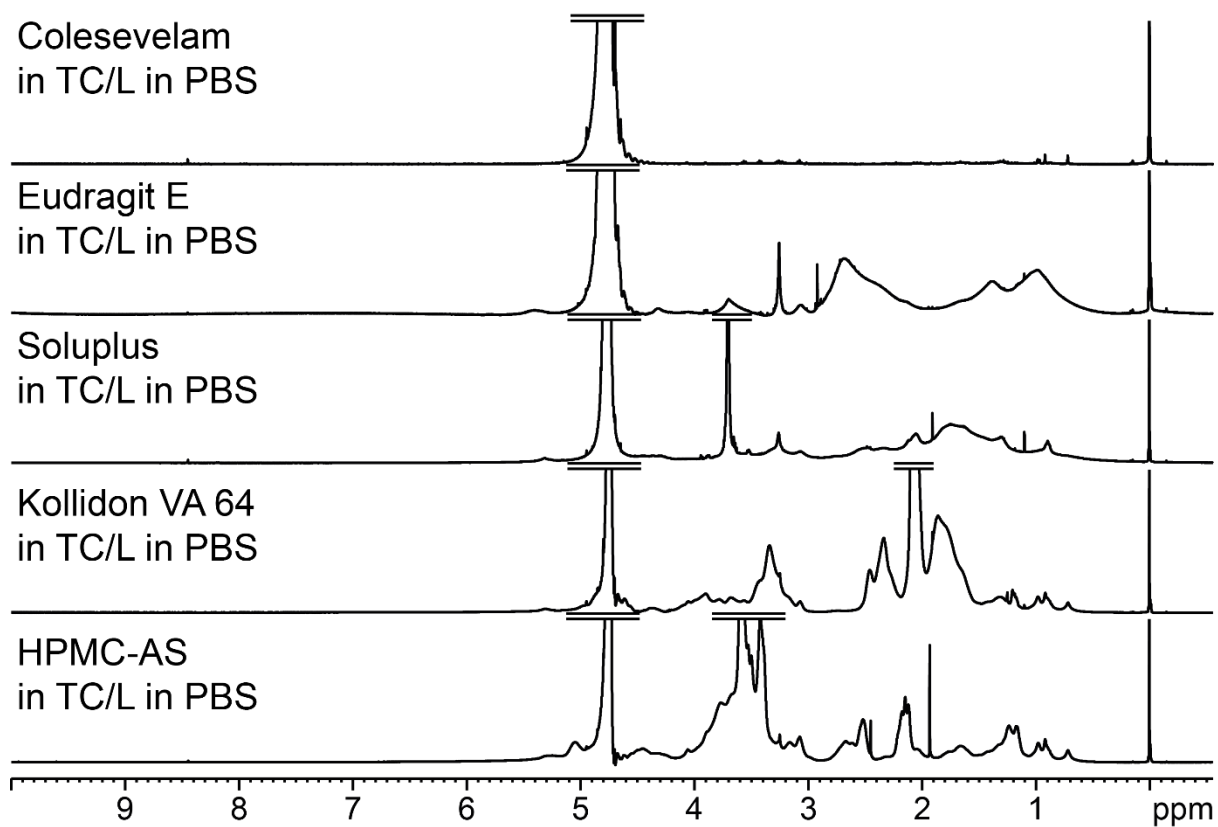


Figure S21: ^1H NMR spectra of 1% Colesevelam, Eudragit E, Soluplus, Kollidon VA 64, and HPMC-AS in TC/L in PBS.

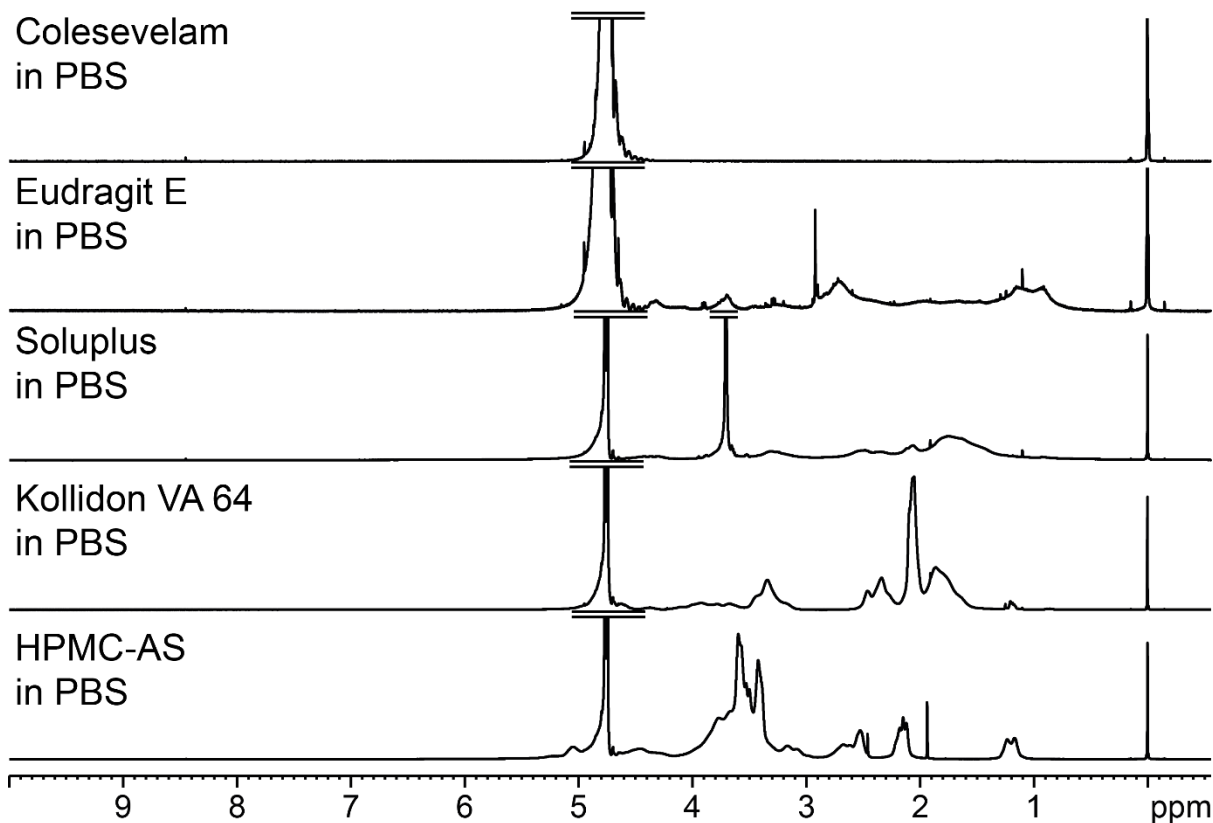


Figure S22: Complete ^1H NMR spectra of 1% Colesevelam, Eudragit E, Soluplus, Kollidon VA 64, and HPMC-AS in PBS.

S4 Polymer impact on free drug

S4.1 Perphenazine ^1H nuclear magnetic resonance (^1H NMR) analysis

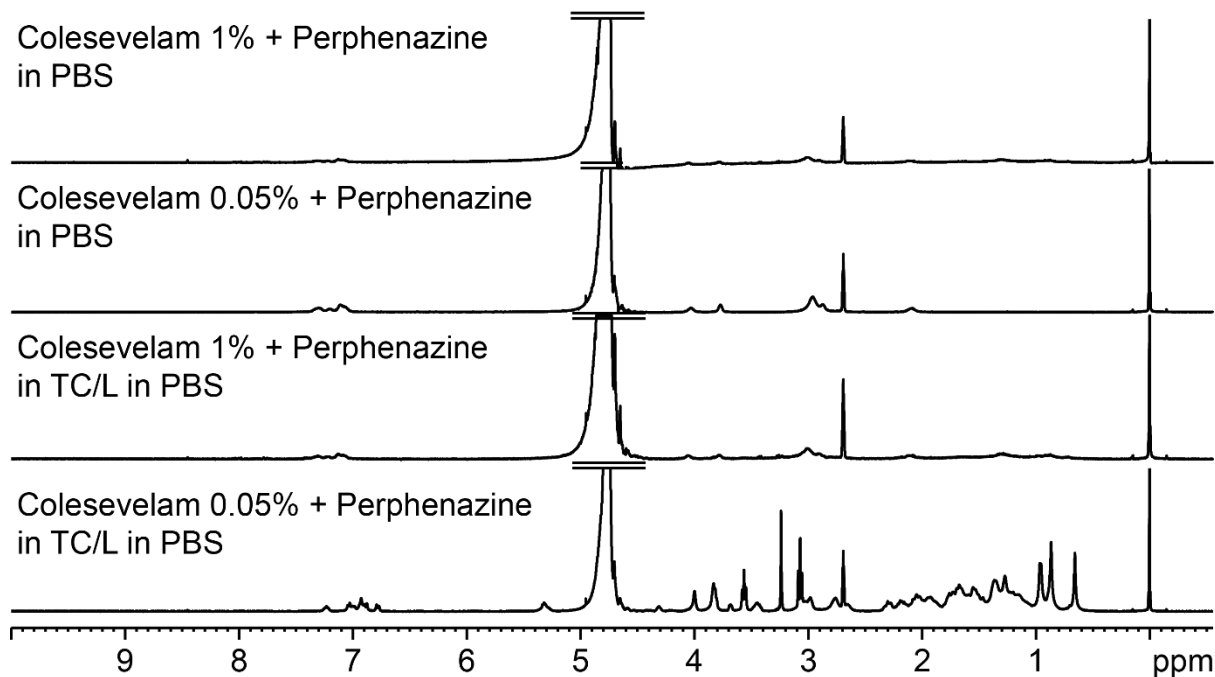


Figure S23: Complete ^1H NMR spectra of Colesevelam with Perphenazine in TC/L in PBS and in PBS.

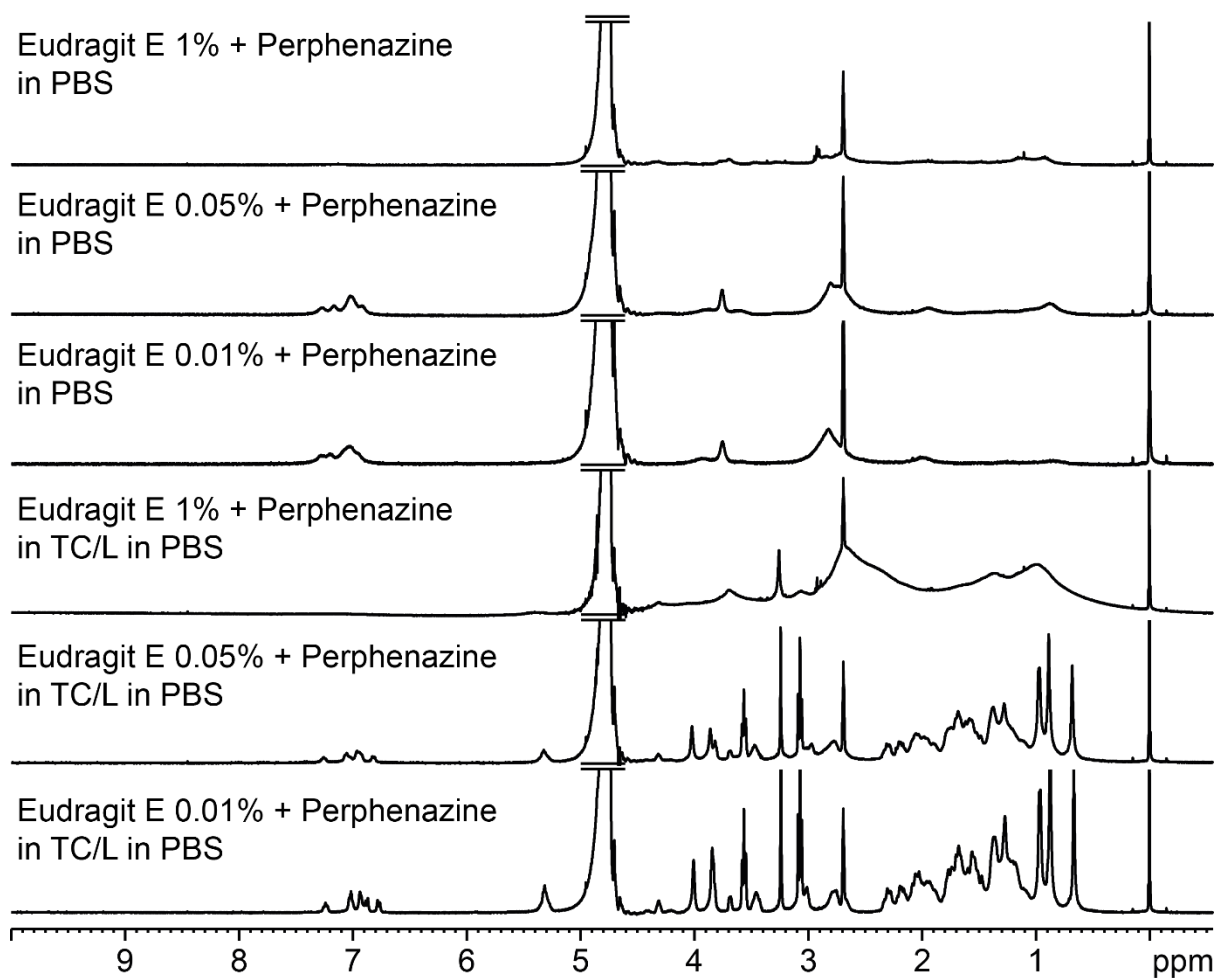


Figure S24: Complete ¹H NMR spectra of Eudragit E with Perphenazine in PBS in TC/L and in PBS.

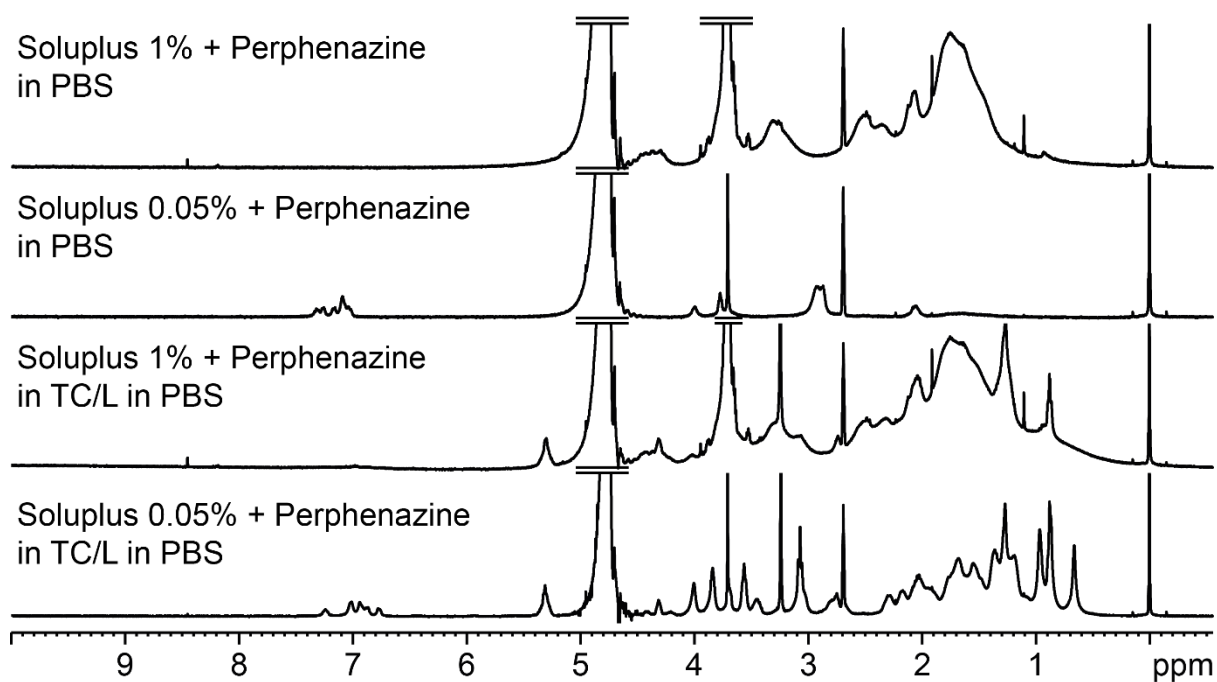


Figure S25: Complete ¹H NMR spectra of Soluplus with Perphenazine in PBS in TC/L and in PBS.

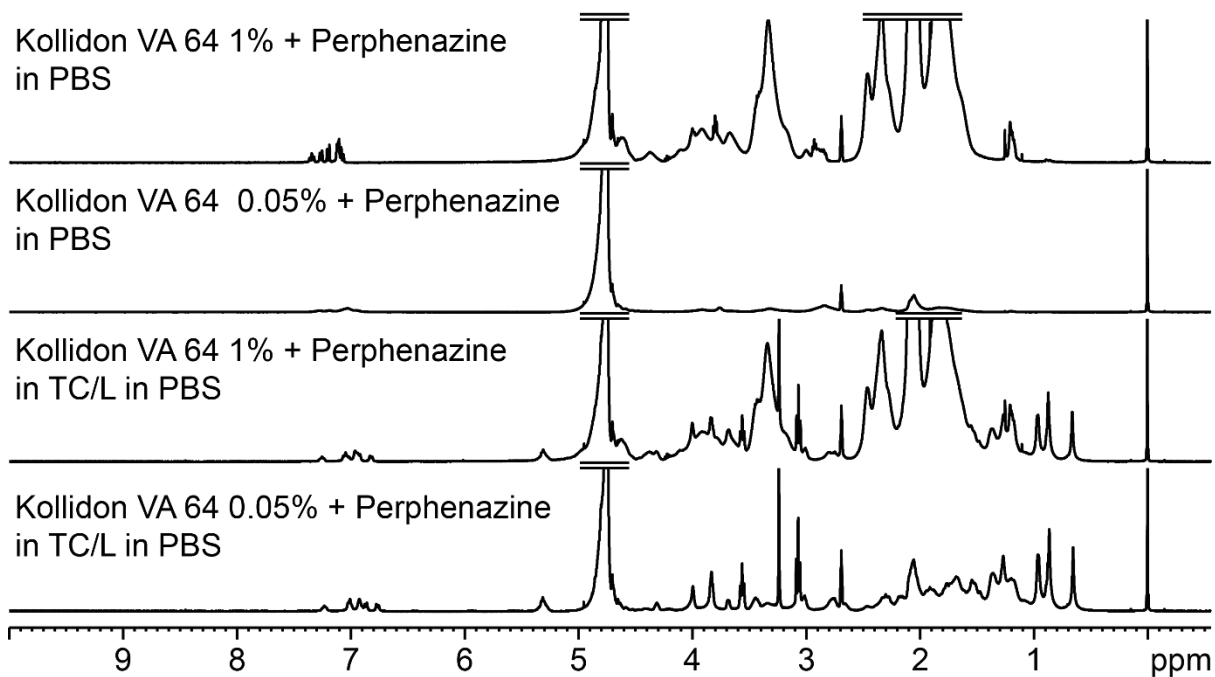


Figure S26: Complete ^1H NMR spectra of Kollidon VA 64 with Perphenazine in PBS in TC/L and in PBS.

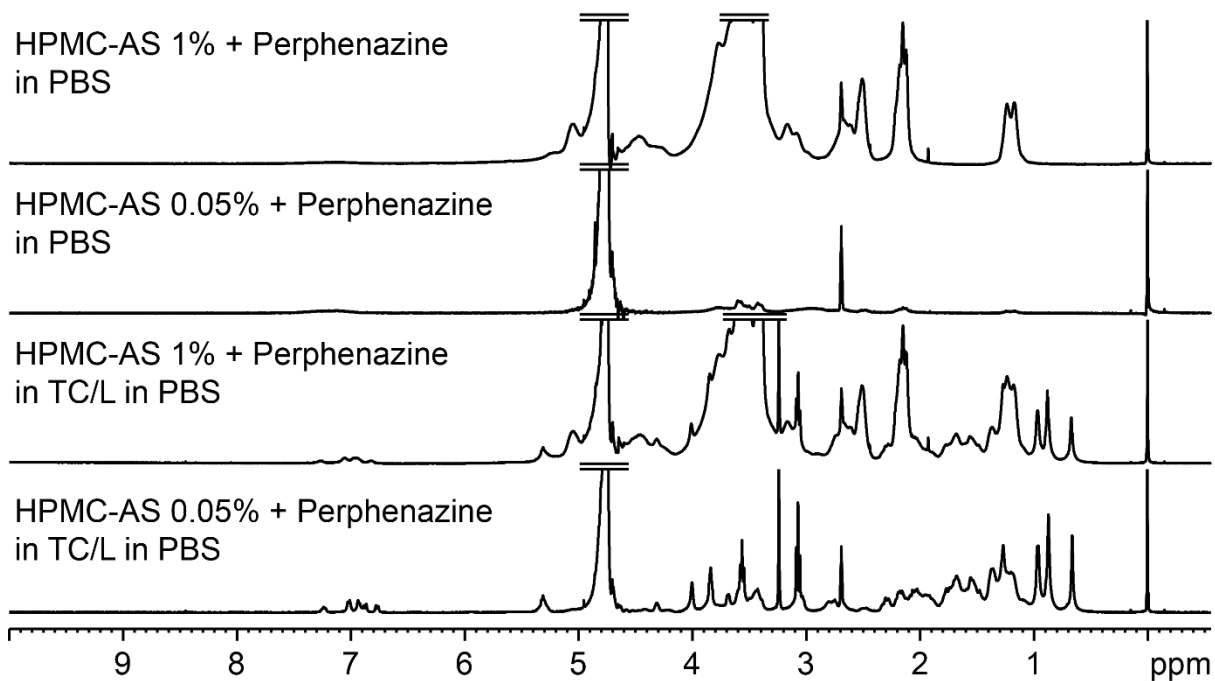


Figure S27: Complete ^1H NMR spectra of HPMC-AS with Perphenazine in PBS in TC/L and in PBS.

S4.2 Imatinib ^1H nuclear magnetic resonance (^1H NMR) analysis

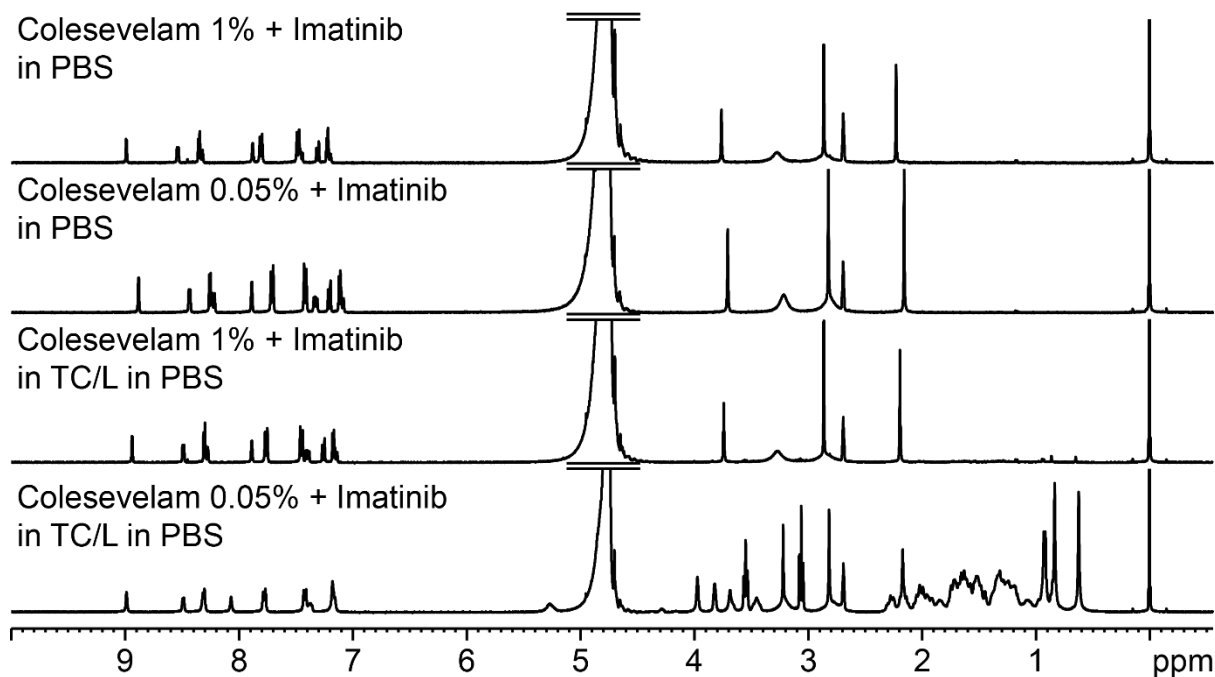


Figure S28: Complete ^1H NMR spectra of Colesevelam with Imatinib in PBS in TC/L and in PBS.

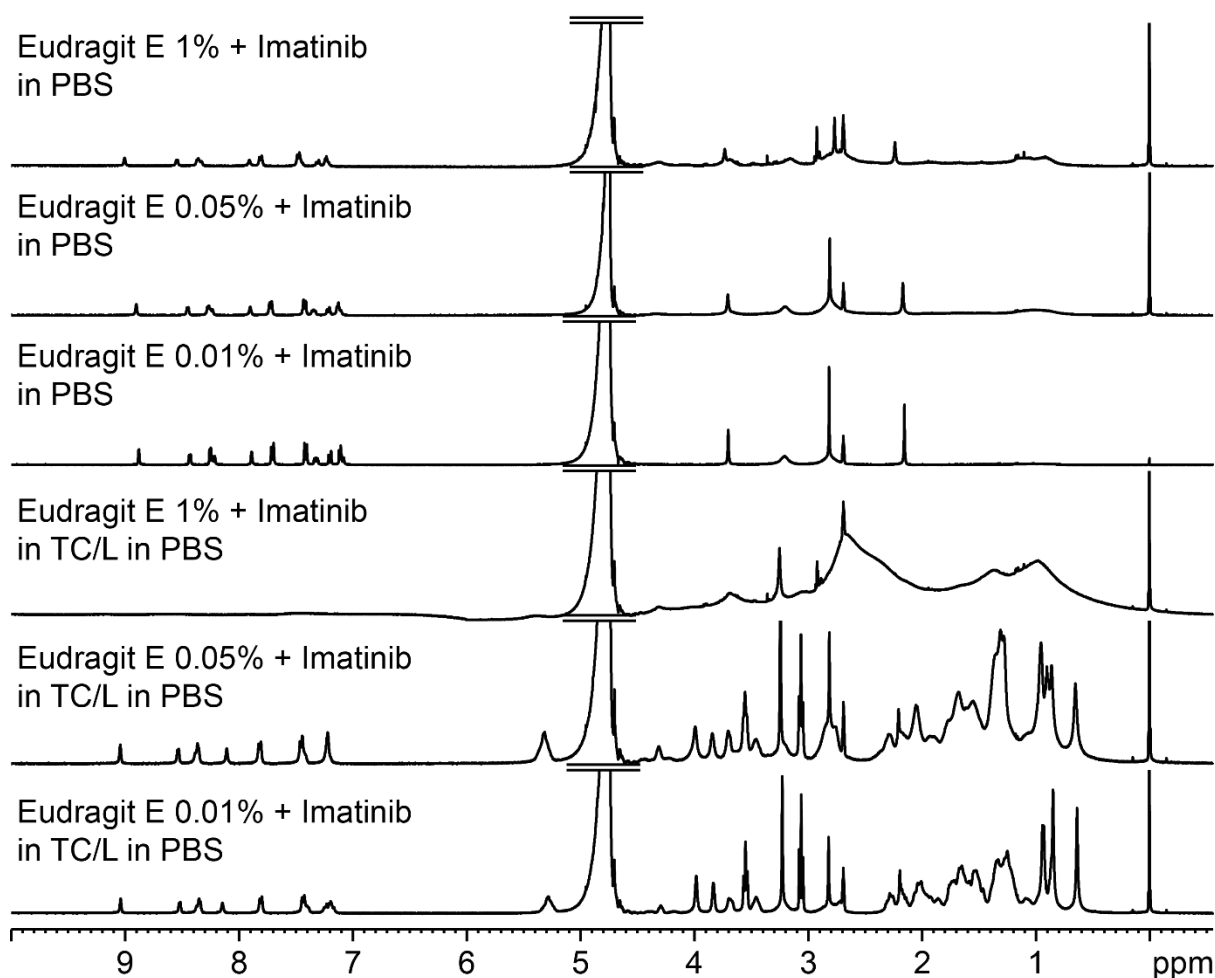


Figure S29: complete ^1H NMR spectra of Eudragit E with Imatinib in PBS in TC/L and in PBS.

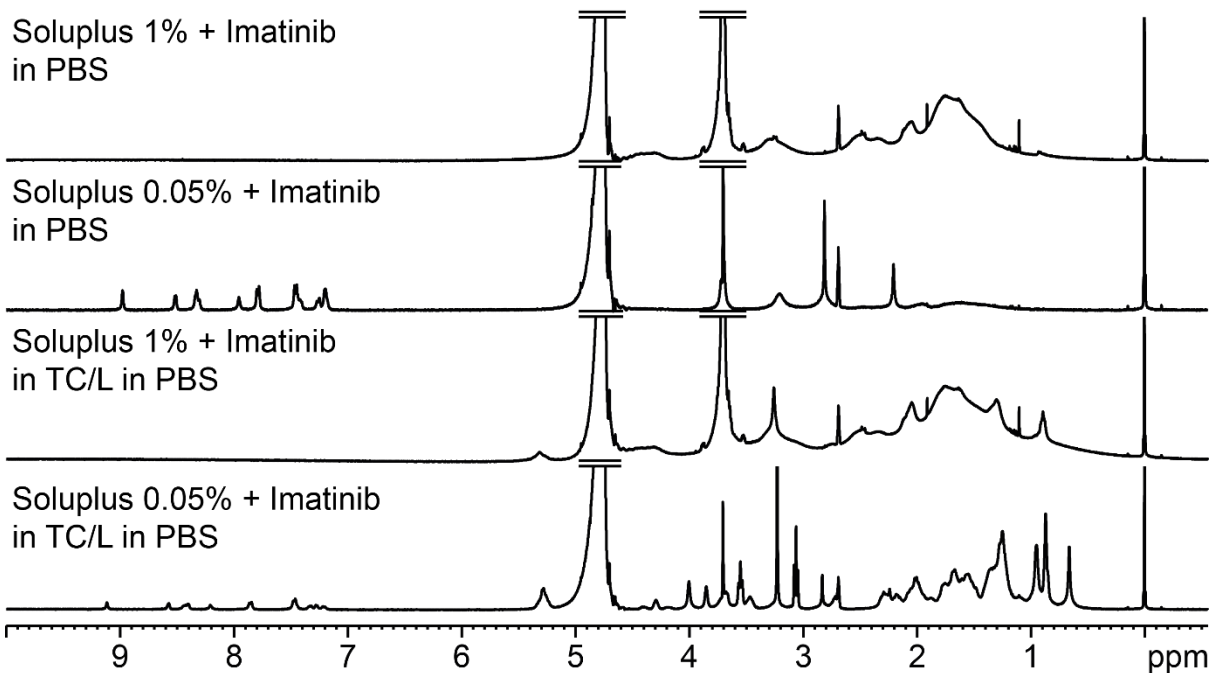


Figure S30: Complete ^1H NMR spectra of Soluplus with Imatinib in PBS in TC/L and in PBS.

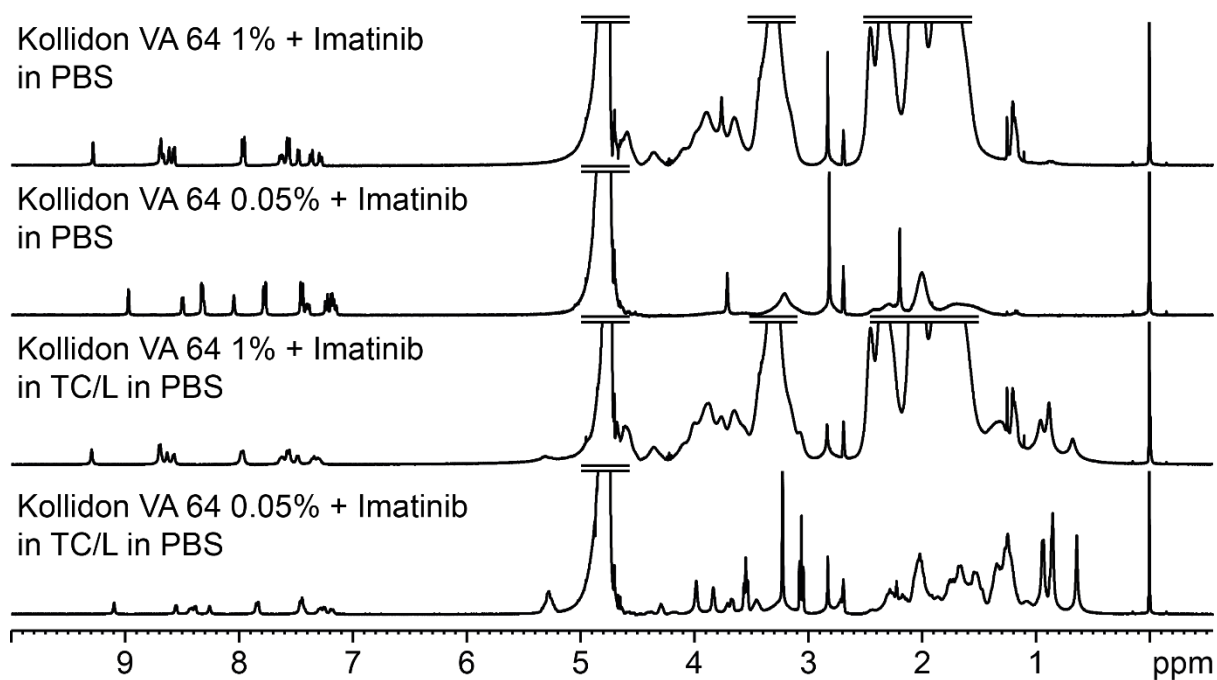


Figure S31: Complete ^1H NMR spectra of Kollidon VA 64 with Imatinib in PBS in TC/L and in PBS.

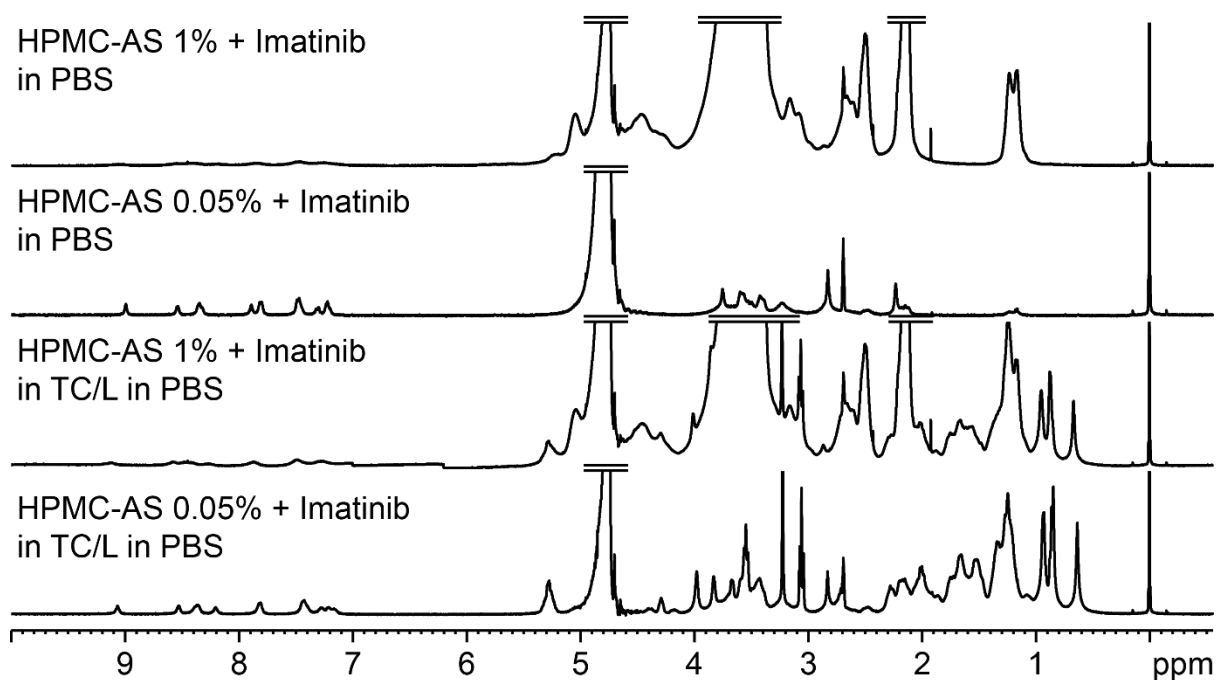


Figure S32: Complete ^1H NMR spectra of HPMC-AS with Imatinib in PBS in TC/L and in PBS.

S4.3 Metoprolol ^1H nuclear magnetic resonance (^1H NMR) analysis

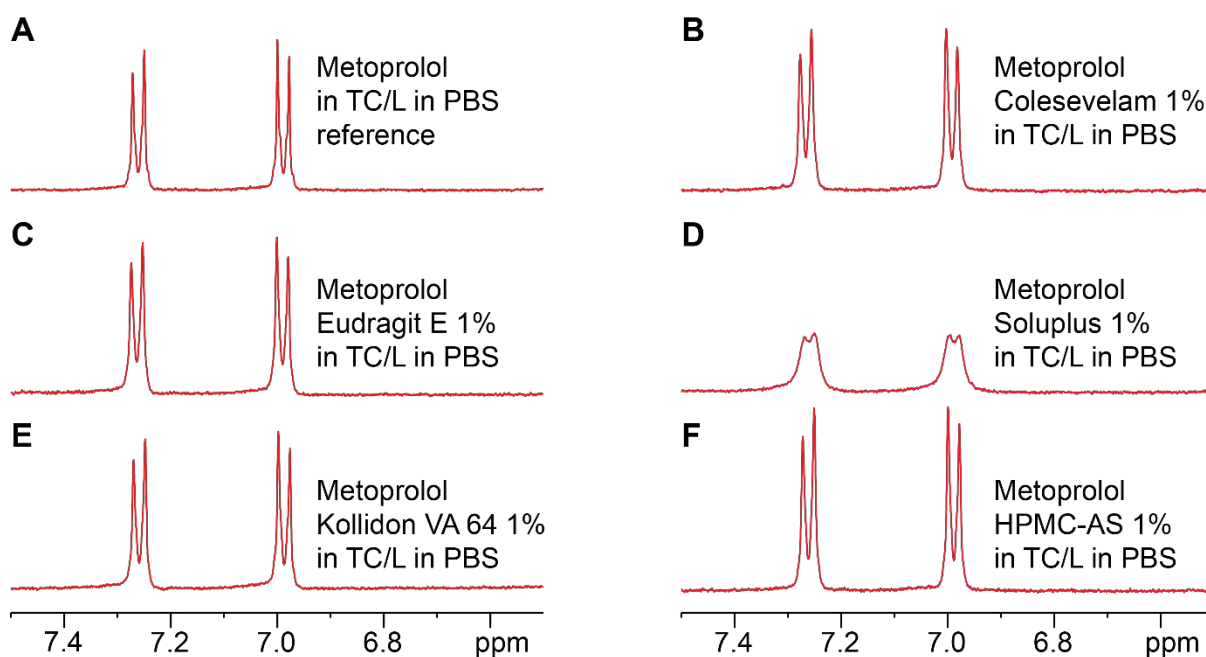


Figure S33: Metoprolol ^1H NMR aryl-proton spectra (A) in TC/L in PBS and with 1% respective polymer in TC/L in PBS (B-F). Metoprolol aryl-proton signals were not impacted by (B) Colesevelam, (C) Eudragit E, (E) Kollidon VA 64, and (F) HPMC-AS at 1% in TC/L in PBS. (D) Signal decreased in intensity and broadened by Soluplus.

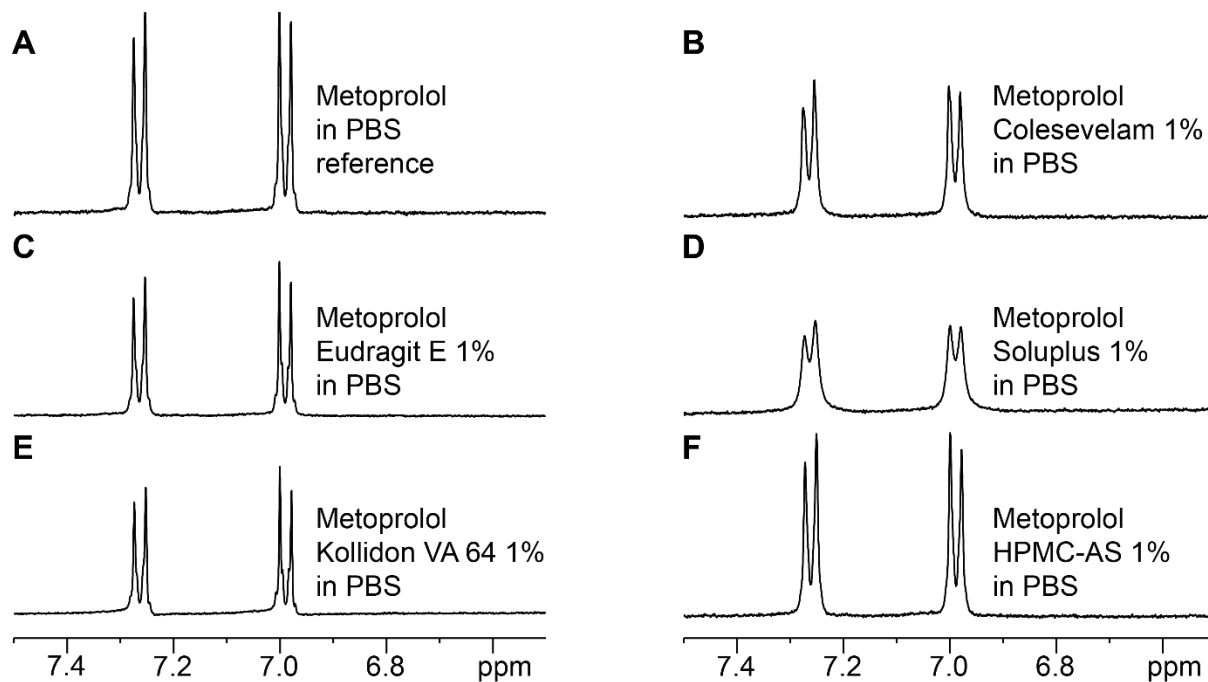


Figure S34: Metoprolol ¹H NMR aryl-proton spectra (A) in PBS and with 1% respective polymer in PBS (B-F). (B) Colesevelam, (C) Eudragit E, (D) Soluplus and (E) Kollidon VA 64 decreased signal intensity in PBS. (D) Soluplus broadened signals. (F) Signals were not impacted by 1% HPMC-AS in PBS.

S5 Polymer impact on HDO diffusivity

Table S4: HDO diffusion coefficients (D in m²/s) for polymers in TC/L in PBS with Perphenazine at 4.703 ppm.

Concentration [%]	Colesevelam		Eudragit E		Soluplus		Kollidon VA 64		HPMC-AS	
	D *10 ⁻⁹	Error by fit *10 ⁻¹¹	D *10 ⁻⁹	Error by fit *10 ⁻¹¹	D *10 ⁻⁹	Error by fit *10 ⁻¹¹	D *10 ⁻⁹	Error by fit *10 ⁻¹¹	D *10 ⁻⁹	Error by fit *10 ⁻¹¹
0.01	N/A	N/A	2.60	0.597	N/A	N/A	N/A	N/A	N/A	N/A
0.05	2.61	9.9	2.56	1.74	2.57	0.745	2.60	0.948	2.60	0.626
1	2.62	0.624	2.58	0.864	2.55	0.318	2.47	3.19	2.52	0.717
0	2.60*10 ⁻⁹ Error by fit: 2.70*10 ⁻¹²									

Table S5: Perphenazine aryl-proton diffusion coefficients (D in m²/s) for polymers (0.05%) in TC/L in PBS at 7.2 and 6.7 ppm. Preliminary data set as signal decay did not reach < 10 % of initial intensity.

Concentration, signal	Colesevelam		Eudragit E		Soluplus		Kollidon VA 64		HPMC-AS	
	D *10 ⁻¹⁰	Error by fit *10 ⁻¹¹	D *10 ⁻¹⁰	Error by fit *10 ⁻¹¹	D *10 ⁻¹⁰	Error by fit *10 ⁻¹¹	D *10 ⁻¹⁰	Error by fit *10 ⁻¹¹	D *10 ⁻¹⁰	Error by fit *10 ⁻¹¹
0.05% 7.2ppm	1.55	2.92	1.12	6.00	0.782	4.46	1.23	2.49	1.22	2.40
0.05% 6.7ppm	1.62	3.09	1.12	4.94	0.538	4.72	1.31	3.04	1.02	2.37
0% 7.2ppm	1.16*10 ⁻¹⁰ Error by fit: 2.10*10 ⁻¹¹									
0% 6.7ppm	1.35*10 ⁻¹⁰ Error by fit: 2.57*10 ⁻¹¹									

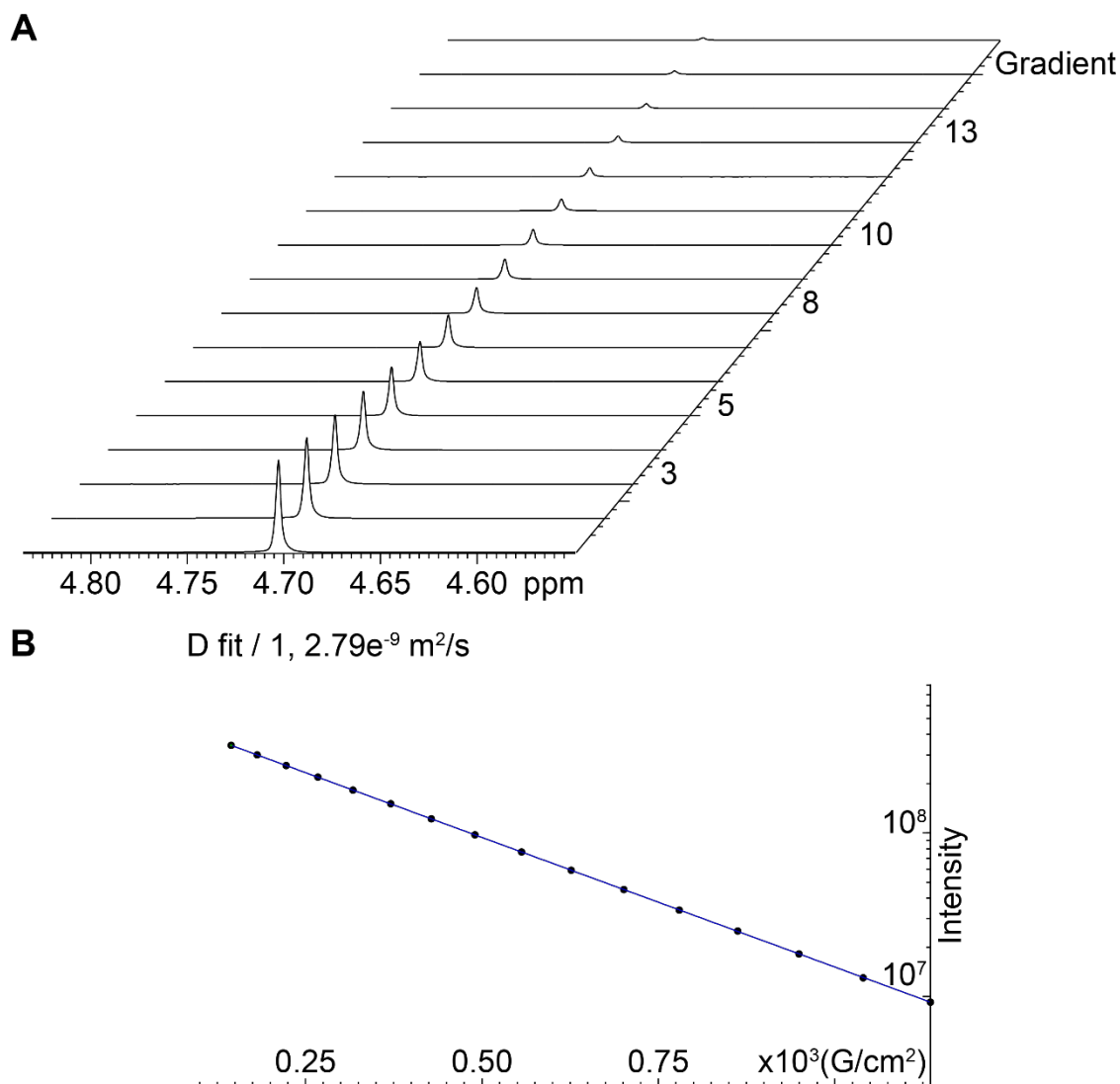


Figure S35: DOSY analysis: (A) HDO (4.703 ppm) signal attenuation with increased gradient strength and (B) fitted curve of experimental intensity decay as a function of the gradient strength for Perphenazine in TC/L in PBS (without polymer).

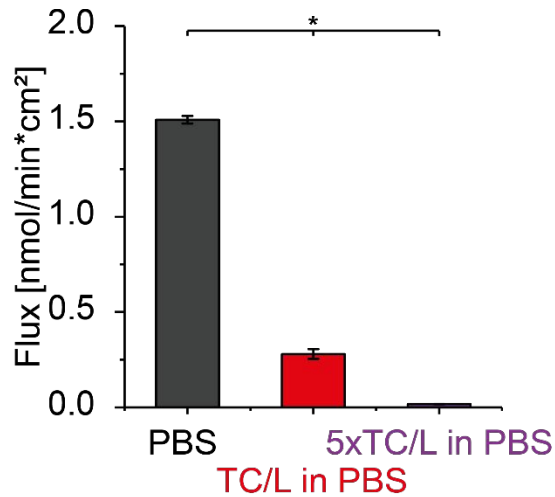
S6 Excipient concentration under physiological conditions

The fluid volume in the fasted small intestine varies between 45 and 319 ml (mean: 107 ± 72 ml), unevenly distributed in roughly four fluid pockets with a median volume of 12 ml [2]. An average oral dosage form contains 280 mg excipients [3]. Hence, dissolving 280 mg excipient in a fluid pocket with a volume of 12 ml results in a mass concentration of 2.33%. For tablet coating, few milligrams of glazing agent are required [4]. Assuming 2 mg coating mass results in a concentration of 0.017%. A tablet is usually composed of more than one excipient, consequently the concentration for one respective excipient is <2.33%. Therefore, our tested polymer concentrations ranging from 0.01-1% reflects the physiological situation.

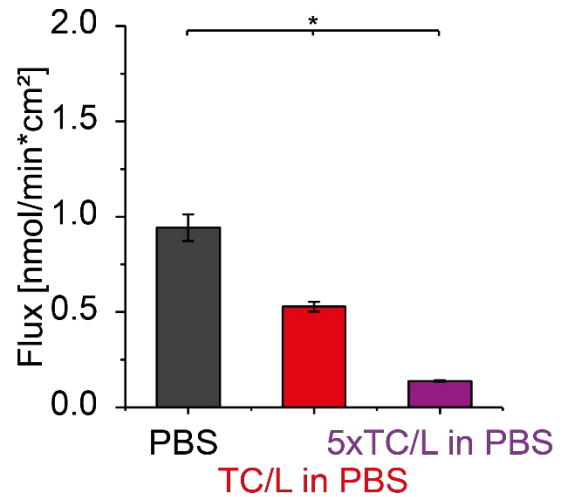
S7 Flux evaluation

S7.1 Flux at different TC/L concentrations

A Perphenazine



B Imatinib



C Metoprolol

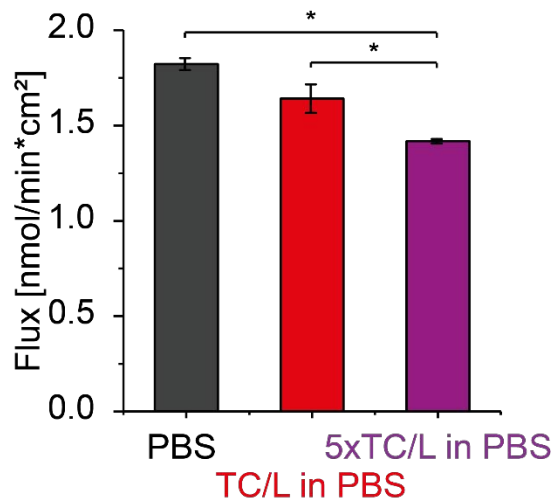
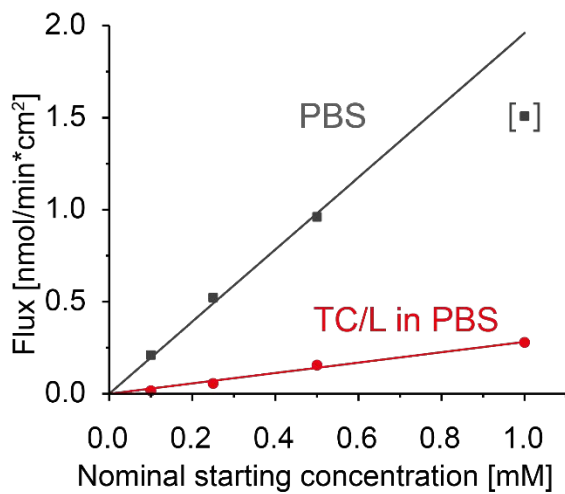


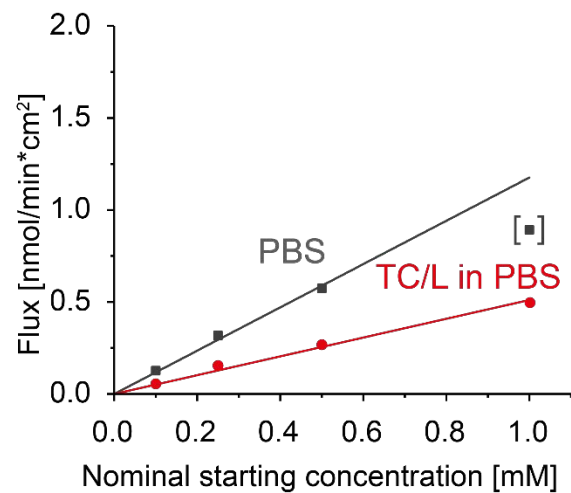
Figure S36: Flux of (A) Perphenazine, (B) Imatinib, and (C) Metoprolol (each at 1000 $\mu\text{mol/l}$) in PBS (black), in TC/L in PBS (red; simulating a fasted state and known as FaSSIF V1, [5]), and in TC/L at fivefold concentration in PBS as compared to FaSSIF V1 (purple; simulating a fed state and known as FeSSIF V1[5]). Flux was significantly reduced for Perphenazine and Imatinib in TC/L in PBS and in 5xTC/L in PBS. Metoprolol flux was not significantly reduced in TC/L in PBS compared to PBS, but in 5xTC/L in PBS. Data shown as mean \pm SD, ANOVA considering $p \leq 0.05$ as statistically significant followed by Games-howell *post-hoc* test for pairwise comparison as the criteria of variance homogeneity was not fulfilled (significant differences are shown by asterisks).

S7.2 Flux at different drug starting concentrations

A Perphenazine



B Imatinib



C Metoprolol

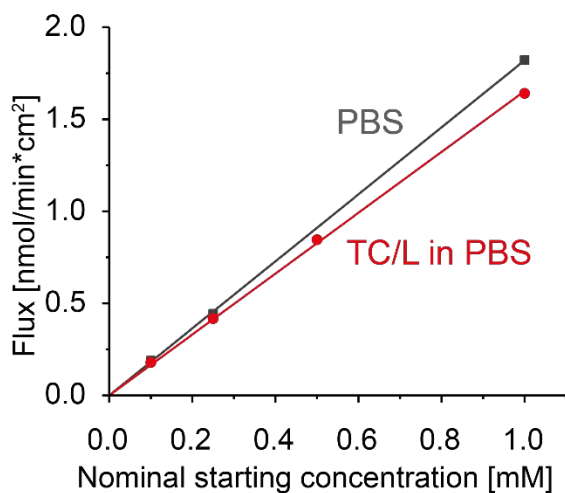
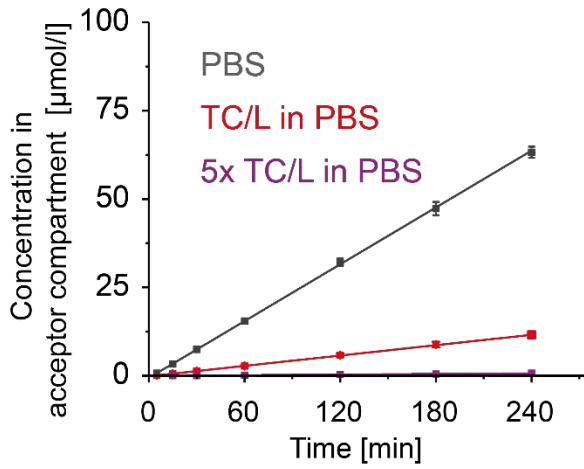


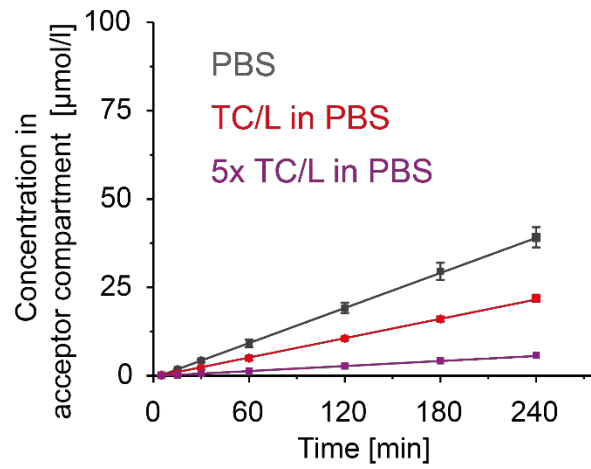
Figure S37: Flux of (A) Perphenazine, (B) Imatinib, and (C) Metoprolol at different starting concentrations (100, 250, 500, and 1000 $\mu\text{mol/l}$) in PBS (black) and in TC/L in PBS (red). Flux increased linearly over concentration in all cases in TC/L in PBS. In PBS at 1000 μM flux for (A) Perphenazine and (B) Imatinib did not follow the linear trend of measurements at low concentrations (data point in brackets). Nevertheless, flux was stable over time for this concentration (**Figure S37**). Data shown as a single point measurement.

S7.3 Drug concentration over time

A Perphenazine



B Imatinib



C Metoprolol

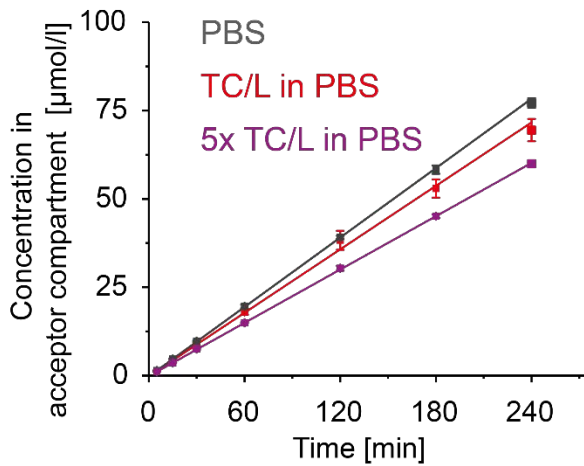


Figure S38: (A) Perphenazine, (B) Imatinib, and (C) Metoprolol concentration [$\mu\text{mol/l}$] in the flux acceptor compartment in PBS (black), in TC/L in PBS (simulating fasted state/FaSSIF V1; red), and with TC/L at fivefold concentration in PBS as compared to FaSSIF V1 (simulating fed state; FaSSIF V1; purple) over time at a starting concentration of 1000 $\mu\text{mol/l}$ in the donor compartment. Concentration increased linearly over time in all cases indicating stable experimental conditions. Data shown as mean \pm SD.

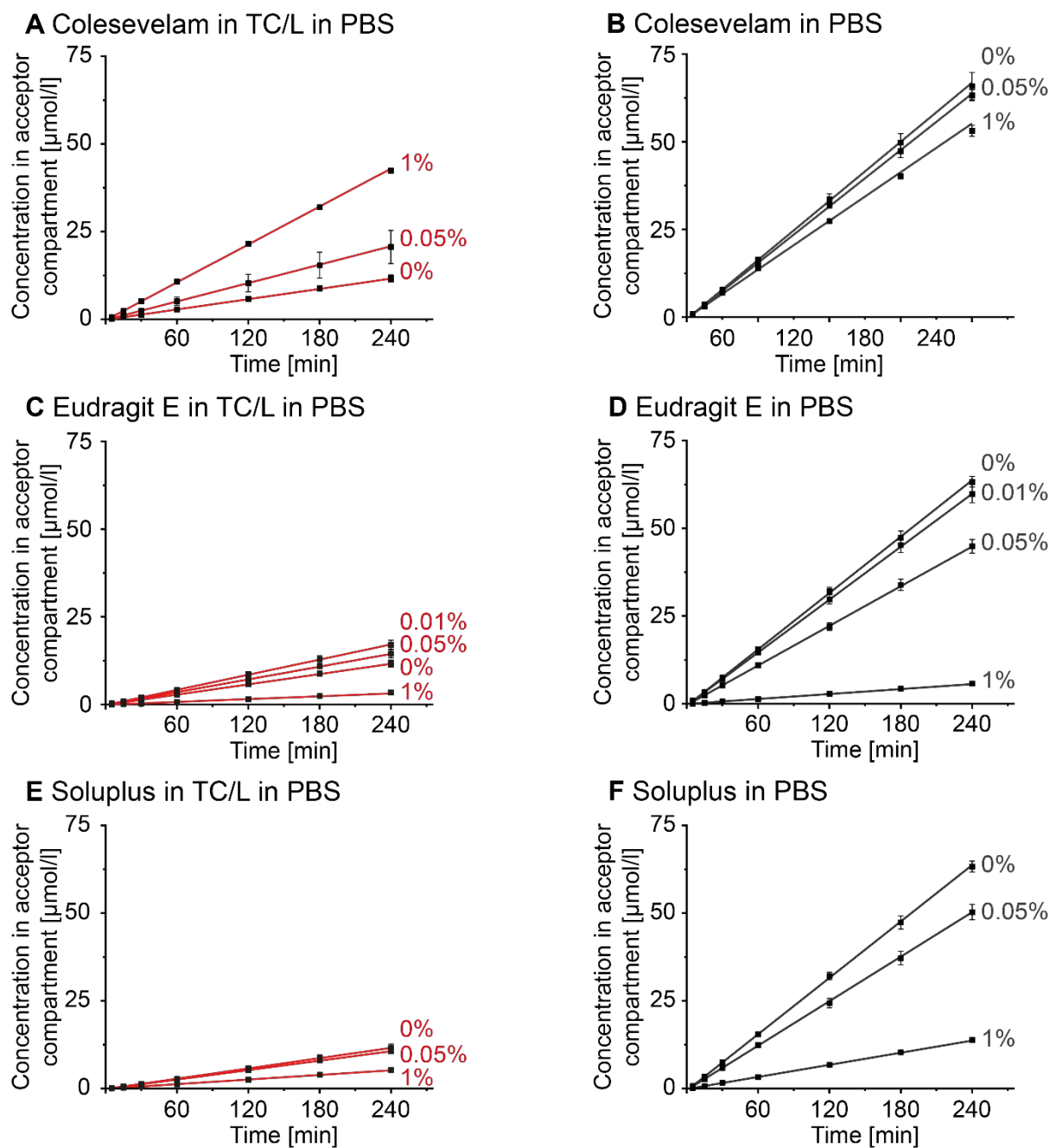


Figure S39: Perphenazine concentration [$\mu\text{mol/l}$] in the flux acceptor compartment over time with (A, B) Colesevelam, (C, D) Eudragit E, (E, F) Soluplus in TC/L in PBS (respective left panel) and in PBS (respective right panel) at concentrations as indicated. Data at 0% polymer concentration are identical for all panels and given for comparison.

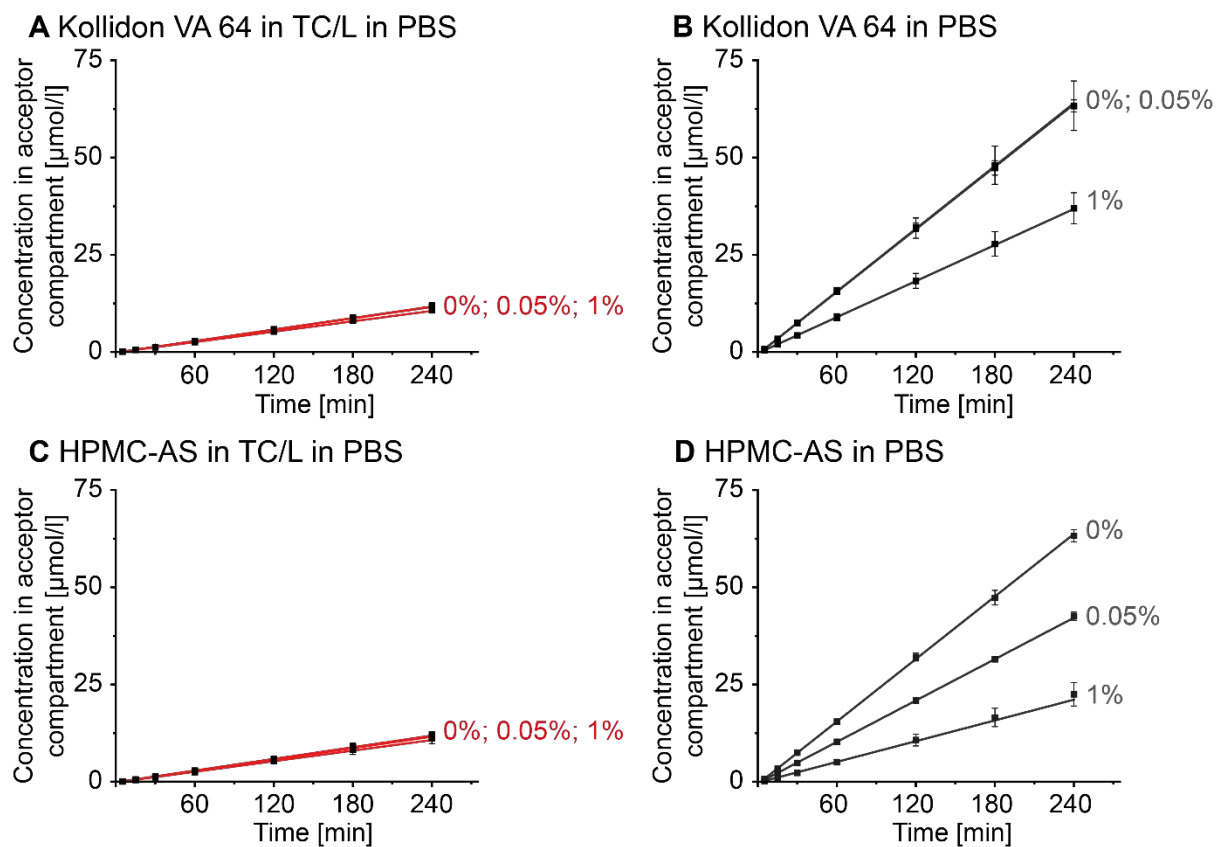


Figure S40: Perphenazine concentration [$\mu\text{mol/l}$] in the flux acceptor compartment over time with (A, B) Kollidon VA 64, (C, D) HPMCAS in TC/L in PBS (respective left panel) and in PBS (respective right panel) at concentrations as indicated. Data at 0% polymer concentration are identical for all panels and given for comparison.

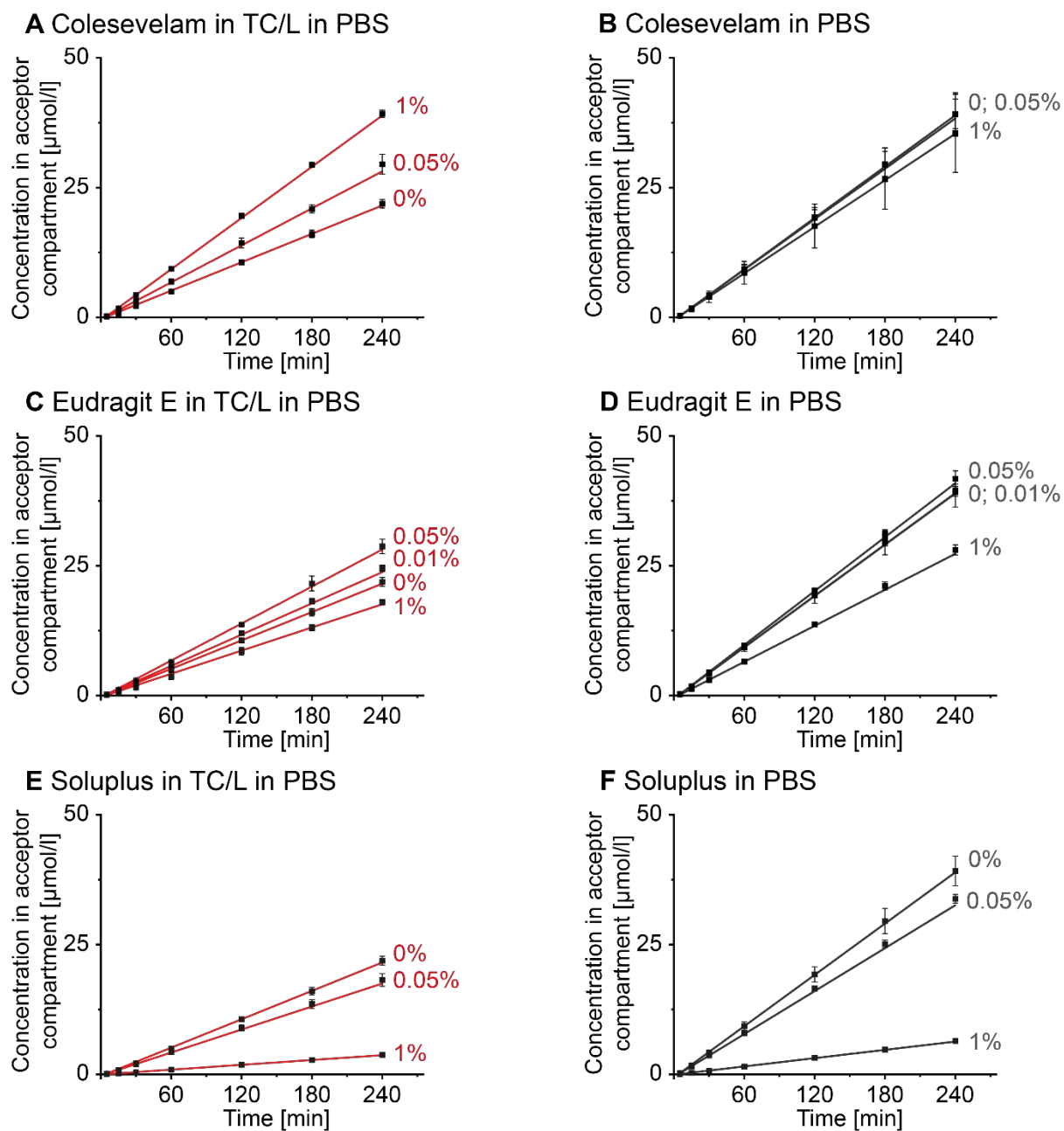


Figure S41: Imatinib concentration [$\mu\text{mol/l}$] in the flux acceptor compartment over time with (A, B) Colesevelam, (C, D) Eudragit E, (E, F) Soluplus in TC/L in PBS (respective left panel) and in PBS (respective right panel) at concentrations as indicated. Data at 0% polymer concentration are identical for all panels and given for comparison

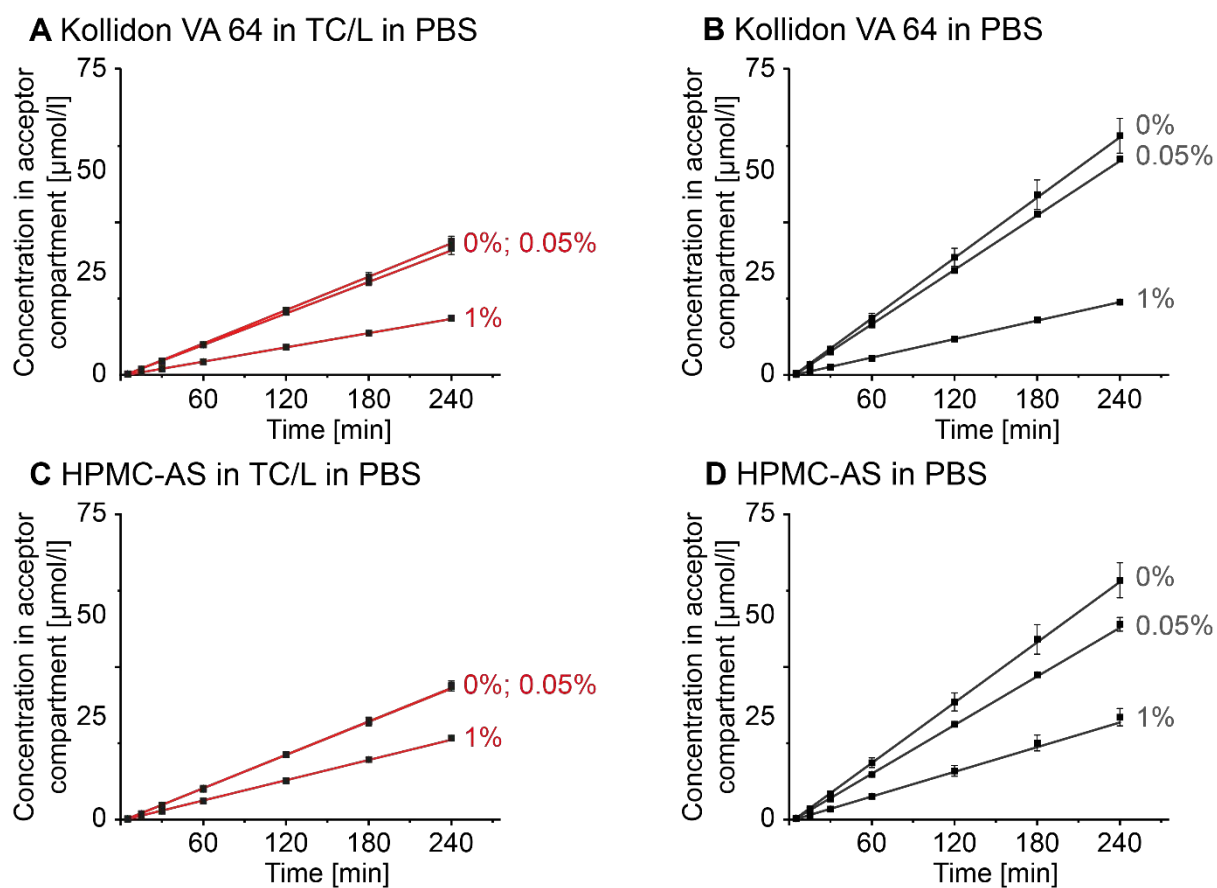


Figure S42: Imatinib concentration [$\mu\text{mol/l}$] in the flux acceptor compartment over time with (A, B) Kollidon VA 64, (C, D) HPMCAS in TC/L in PBS (respective left panel) and in PBS (respective right panel) at concentrations as indicated. Data at 0% polymer concentration are identical for all panels and given for comparison.

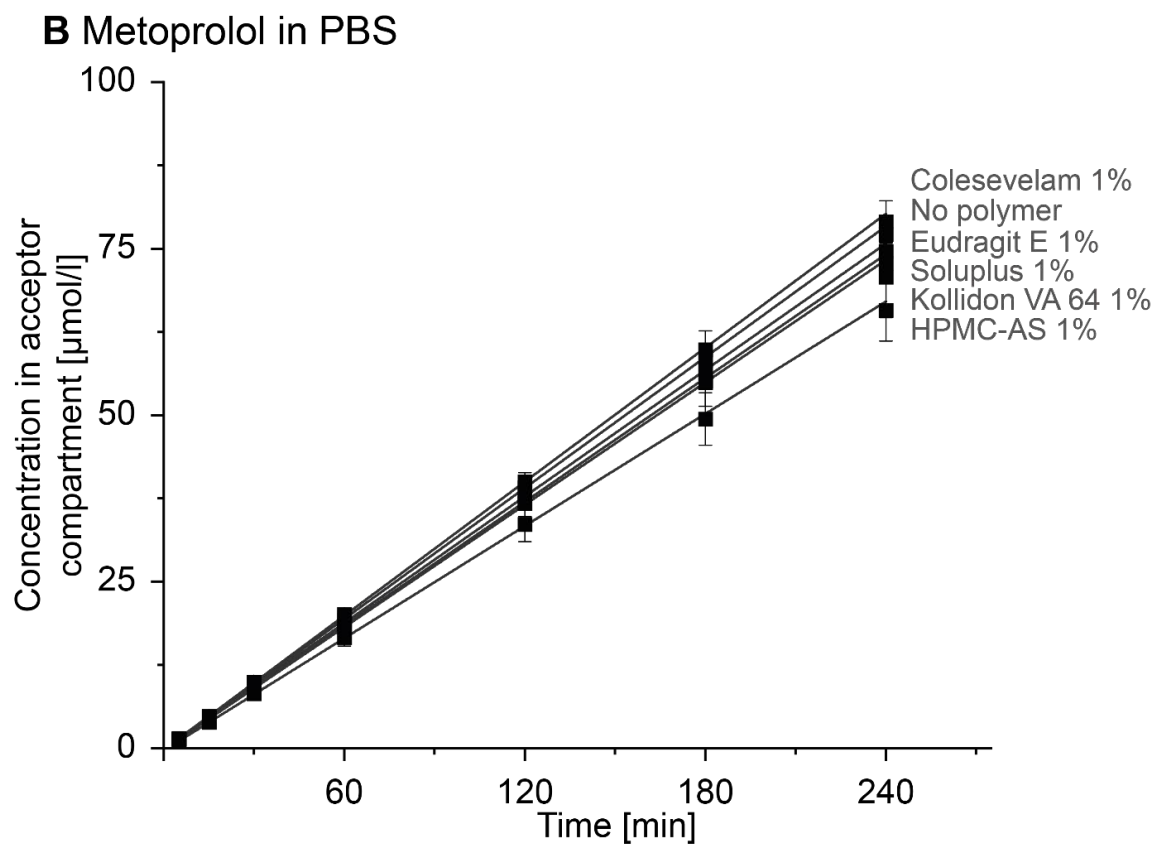
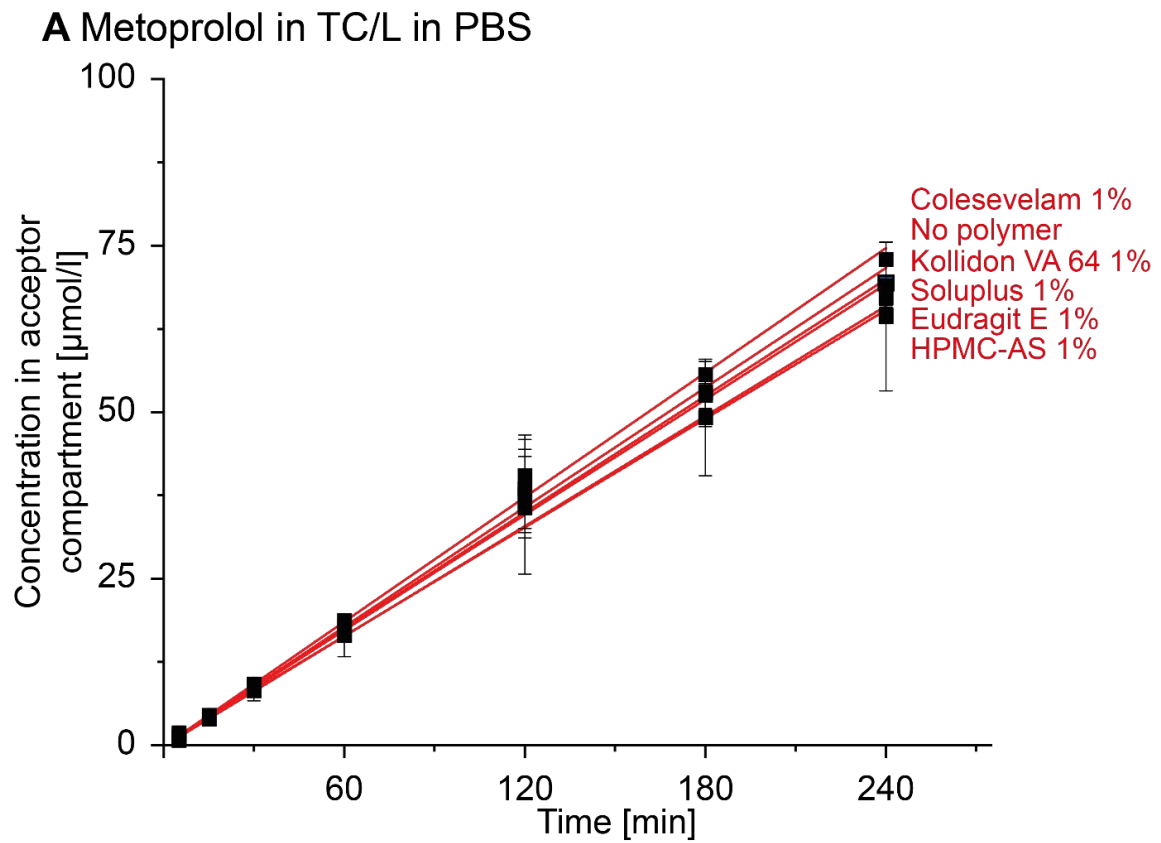


Figure S43: Metoprolol concentration [$\mu\text{mol/l}$] in the flux acceptor compartment over time with polymers as indicated (A) in TC/L in PBS and (B) in PBS at 1% polymer concentration. Data at 0% polymer concentration are provided in each panel.

S7.4 Flux lag time

S7.4.1 Lag time Perphenazine

Initial experiments were conducted at $n = 3$, thereby not allowing reasonable outlier testing. For the four groups with larger standard deviation as outlined in the table below, three additional experiments were conducted and outlier tests were performed. Subsequently, the lag time of these groups were evaluated (**Table S6**). One lag time observation for Perphenazine in PBS was categorized as an outlier based on a double-sided Grubb's outlier test and consequently excluded from the statistical analysis (**Figure S44**).

Table S6: Double-sided Grubb's outlier test for lag time of Perphenazine in PBS, in TC/L in PBS, in TC/L in PBS with 1% Eudragit E, and in TC/L in PBS with 1% HPMC-AS with a significance level of 0.05. One outcome was excluded as highlighted in bold/italic numbers.

Number	Lag time Perphenazine in PBS [min]	Lag time Perphenazine in TC/L in PBS [min]	Lag time Perphenazine in TC/L in PBS with 1% Eudragit E [min]	Lag time Perphenazine in TC/L in PBS with 1% HPMC-AS [min]
1	3,05	3,75	13,98	5,63
2	2,70	3,06	13,49	9,90
3	-0,13	1,81	16,66	5,50
4	2,84	5,93	8,57	7,76
5	2,24	5,62	12,21	7,29
6	2,60	5,77	8,73	7,52
Result from Grubb's-test	Outlier (-0,13)	No Outlier	No Outlier	No Outlier

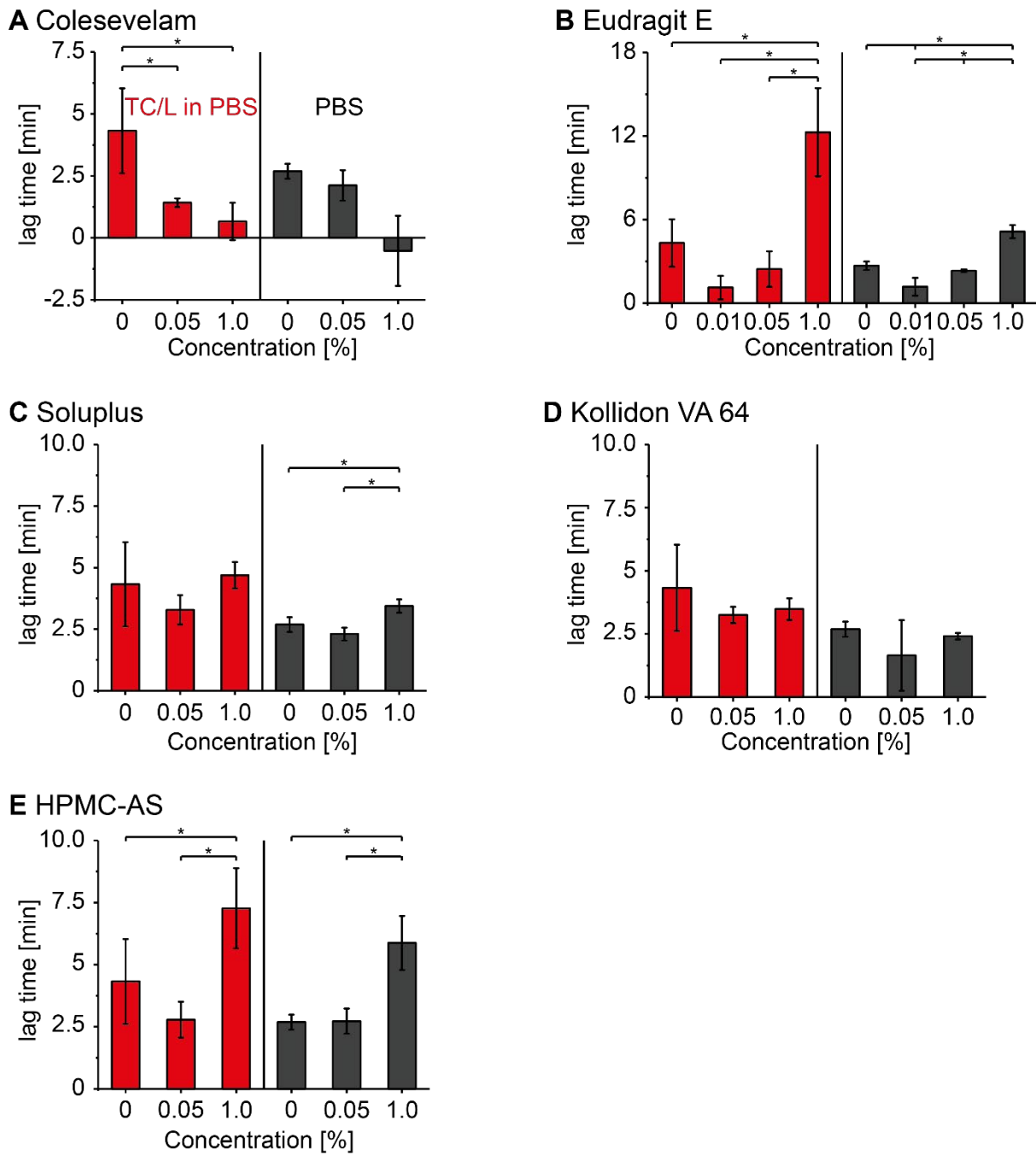


Figure S44: Lag time of Perphenazine with (A) Colesevelam, (B) Eudragit E, (C) Soluplus, (D) Kollidon VA 64, and (E) HPMC-AS in TC/L in PBS (red) and in PBS (black) at concentrations as indicated. The data reported at 0% are identical for all panels and given for comparison. Data for (B) Eudragit E is also shown in Figure 6 in the manuscript. Lag time was calculated by time axis intersect of the extrapolated linear part (**Figure S36**). Data shown as mean \pm SD, ANOVA considering $p \leq 0.05$ as statistically significant followed by Tukey post-hoc test for pairwise comparison (significant differences are shown by asterisks).

S7.4.2 Lag time Imatinib

Due to a very high lag time standard deviation of some samples, outlier tests were performed. Lag time of Imatinib in TC/L in PBS, in TC/L in PBS with 1% Eudragit E, in TC/L in PBS with 1% Soluplus, and in TC/L in PBS with 1% HPMC-AS was reevaluated with three additional experimental repetitions (**Table S7**). As a result, one lag time data point for Imatinib in TC/L in PBS was removed from further statistical analysis (**Figure S45**).

Table S7: double-sided Grubb's outlier test for lag time of Imatinib in TC/L in PBS, in TC/L in PBS with 1% Eudragit E, in TC/L in PBS with 1% Soluplus, and in TC/L in PBS with 1% HPMC-AS with a significance level of 0.05. One outcome was excluded as highlighted in bold/italic numbers.

Number	Lag time Imatinib in TC/L in PBS [min]	Lag time Imatinib in TC/L in PBS with 1% Eudragit E [min]	Lag time Imatinib in TC/L in PBS with 1% Soluplus [min]	Lag time Imatinib in TC/L in PBS with 1% HPMC-AS [min]
1	3,32	8,33	4,02	6,99
2	3,68	5,10	1,23	2,34
3	12,16	14,74	2,46	6,16
4	5,11	6,45	6,15	8,56
5	5,54	8,62	6,63	6,22
6	5,03	8,88	5,33	8,49
Result from Grubb's-test	Outlier (12,16)	No Outlier	No Outlier	No Outlier

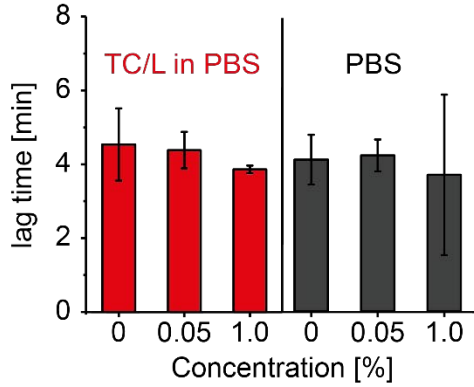
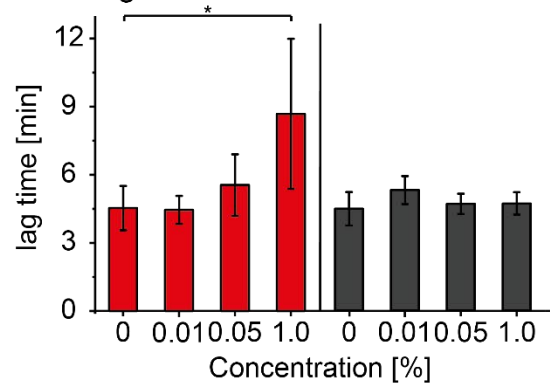
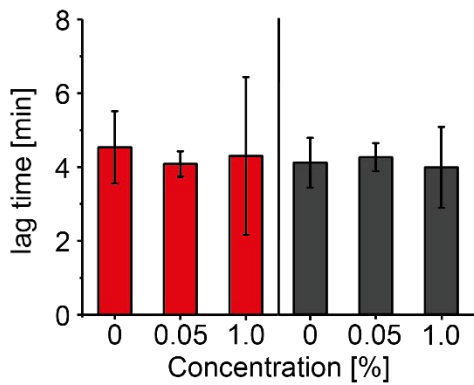
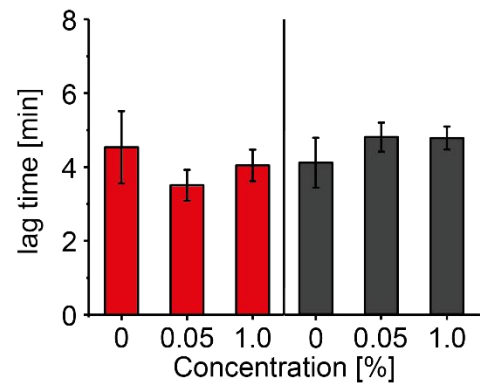
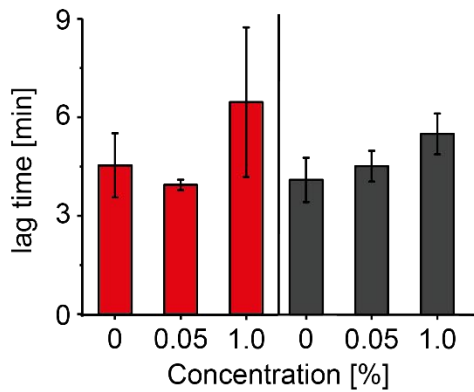
A Colesevelam**B Eudragit E****C Soluplus****D Kollidon VA 64****E HPMC-AS**

Figure S45: Lag time of Imatinib with (A) Colesevelam, (B) Eudragit E, (C) Soluplus, (D) Kollidon VA 64, and (E) HPMC-AS in TC/L in PBS (red) and in PBS (black) at concentrations as indicated. The first bars 0% are identical for all panels and for comparison. Data for (B) Eudragit E is also shown in Figure 6 in the manuscript. Lag time was calculated by time axis intersect of linear concentration over time extrapolation (**Figure S36**). Data shown as mean \pm SD, ANOVA considering $p \leq 0.05$ as statistically significant followed by Tukey post-hoc test for pairwise comparison (significant differences are shown by asterisks).

S7.4.3 Lag time Metoprolol

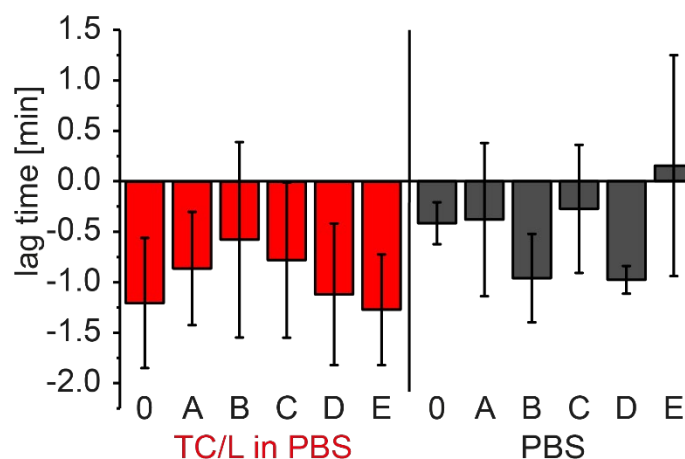


Figure S46: Metoprolol lag time (0) in absence of polymer, with 1% (A) Colesevelam, (B) Eudragit E, (C) Soluplus, (D) Kollidon VA 64, and (E) HPMC-AS in TC/L in PBS (red) and in PBS (black). No difference in lag time between the groups was observed.

S8 Imatinib flux reduction by polymer presence

Flux reduction was calculated at 1% polymer concentration as follows (Eq.1).

$$\text{Flux reduction [\%]} = \left(1 - \frac{\text{Flux}_{1\% \text{ polymer in TC/L in PBS}}}{\text{Flux}_{1\% \text{ polymer in PBS}} \right) * 100 \quad \text{Eq. 1}$$

Imatinib flux in Kollidon VA 64 and HPMC-AS presence was decreased by 23.0% and 20.8%, respectively. In contrast, Eudragit E and Soluplus decreased flux by 35.2% and 42.0%, respectively. This indicated higher affinity of Imatinib to TC/L/polymer MIM than to coexisting species.

References

- [1] J. Wiest, M. Saedtler, B. Böttcher, M. Grüne, M. Reggane, B. Galli, U. Holzgrabe, L. Meinel, Geometrical and Structural Dynamics of Imatinib within Biorelevant Colloids, *Mol. Pharm.*, 15 (2018) 4470-4480.
- [2] C. Schiller, C.P. Fröhlich, T. Giessmann, W. Siegmund, H. Monnikes, N. Hosten, W. Weitschies, Intestinal fluid volumes and transit of dosage forms as assessed by magnetic resonance imaging, *Aliment. Pharmacol. Ther.*, 22 (2005) 971-979.
- [3] D. Reker, S.M. Blum, C. Steiger, K.E. Anger, J.M. Sommer, J. Fanikos, G. Traverso, "Inactive" ingredients in oral medications, *Sci. Transl. Med.*, 11 (2019).
- [4] Evonik Nutrition and Care GmbH, Eudragit Polymers for immediate release. <https://healthcare.evonik.com/product/health-care/en/products/pharmaceutical-excipients/immediate-release/>, 2020 (accessed 01 April 2020).
- [5] J.E. Boni, R.S. Brickl, J. Dressman, M.L. Pfefferle, Instant FaSSIF and FeSSIF—Biorelevance Meets Practicality, *Dissolut. Technol.*, 16 (2009) 41-45.